UNIVERSITY OF CALIFORNIA
RIVERSIDE

Data-Driven Intelligent Charging Models and Innovative Pricing Strategies for Managing Electric Vehicles

A Dissertation submitted in partial satisfaction
of the requirements for the degree of

Doctor of Philosophy

in

Electrical Engineering

by

Jacqueline V. Garrido Escobar

December 2023

Dissertation Committee:

Dr. Matthew J. Barth, Chairperson
Dr. Kanok Boriboonsomsin
Dr. Hamed Mohsenian-Rad

The Dissertation of Jacqueline V. Garrido Escobar is approved:

Committee Chairperson

University of California, Riverside

Acknowledgments

I would like to sincerely thank my Ph.D. advisors, Prof. Barth and Dr. Boriboonsomsin. Over the almost four years that I spent at the Transportation System Research (TSR) and Sustainable Integrated Grid Initiative (SIGI) groups at UCR, they provided invaluable advice concerning both my research and future career paths. I am also grateful to all the students from the UCR EcoCAR Challenge team. Working with them on this exciting project is definitely one of the highlights of my time at UCR. I learned to collaborate with students from diverse backgrounds, work in a fast-paced environment, and to unite for a common goal. Additionally, I would like to thank to the students and faculty of the Science to Policy Certificate course. I gained significant insights about the policy making process, which definitely helped me to understand and link my research with past, current, and future policy developments.

I wish to acknowledge the Department of Electrical and Computer Engineering at UCR, the College of Engineering-Center for Environmental Research and Technology (CE-CERT) at UCR, the United States Department of Transportation, the National Center for Sustainable Transportation (NCST), and the U.S. Department of Energy's Advanced Vehicle Technology Competition for their support in my study and research for this dissertation.

To my Victoria.

ABSTRACT OF THE DISSERTATION

Data-Driven Intelligent Charging Models and Innovative Pricing Strategies for Managing Electric Vehicles

by

Jacqueline V. Garrido Escobar

Doctor of Philosophy, Graduate Program in Electrical Engineering
University of California, Riverside, December 2023
Dr. Matthew J. Barth, Chairperson

In order to achieve carbon neutrality in California by 2045, it is estimated that California will need approximately eight million light-duty (LD) electric vehicles (EVs) and 1.5 million shared EV chargers by 2030. Moreover, a specific target has been set to ensure all drayage trucks operating in the state are zero emission (ZE) vehicles by 2035. Aligning EV charging with renewable energy sources and local grid requirements demands innovative charging solutions. Achieving this target will require precise modeling to determine the number, locations, and load characteristics of the EV chargers, especially for the medium-duty (MD) and heavy-duty (HD) vehicle sectors.

This dissertation introduces new novel data-driven coordination techniques through intelligent controlled charging applied to drayage trucks operations and indirect controlled charging by proposing innovative pricing strategies for LD, MD, and HD EVs. It presents a real-time, carbon-based pricing model for EV charging. This model prioritizes periods of high renewable energy availability, considers local solar photovoltaics (PV) variations, and incorporates a Time-of-Use (TOU) pricing structure. Utilizing Machine Learning (ML), it

predicts day-ahead and three-hour-ahead forecasts.

Moreover, this research extensively explores trip- and tour-patterns of battery electric trucks (BETs) in drayage operations. By developing data-driven clustering techniques, this study adjusts energy efficiency values for loaded and unloaded conditions, simulates charging scenarios to determine the state-of-charge (SOC), and presents case studies for potential en-route opportunity charging at specific power levels. An intelligently controlled charging model for BETs is also developed, aiming to optimize tour completion and reduce charging costs using TOU energy rates. Based on a one-year analysis of real-world activity data from a fleet operating at the Ports of Los Angeles and Long Beach, the effectiveness of the algorithm was validated through a sensitivity analysis comparing reserved SOC scenarios of 5%, 50%, and 80%.

The research findings conclude that intelligent charging models paired with innovative pricing strategies can go a long way to help optimize EV charging coordination techniques for EV fleets, reduce energy costs, and address delay costs associated with drayage operations. The study highlights the importance of considering the variability of renewable energy sources and the need for effective coordination between LD/MD/HD charging, port operations, and TOU charging rates.

Contents

List of Figures

List of Tables

Chapter 1

Introduction

According to the US greenhouse gas (GHG) emissions from the Environmental Protection Agency (EPA), the transportation sector was the largest source of global warming emissions inventory, 28% of all emissions, in 2021 [10]. As shown in Figure 1.1 the transportation sector accounts for approximately 40% of the total GHG emissions in California, making it the largest source according to the 2022 inventory report by the California Air Resources Board (CARB) [1].

In addition to being the largest source of GHG emissions, the transportation sector is also responsible for a significant portion of air pollutants such as oxides of nitrogen (NOx) and particulate matter (PM), which pose health risks such as asthma, heart attacks, and cancer [11, 12].

Not all the vehicles pollute the same, so vehicle emissions are usually categorized and evaluated by vehicle class. Vehicle classes are based on gross vehicle weight rating (GVWR) which is explained as the maximum weight of the vehicle as specified by the man-

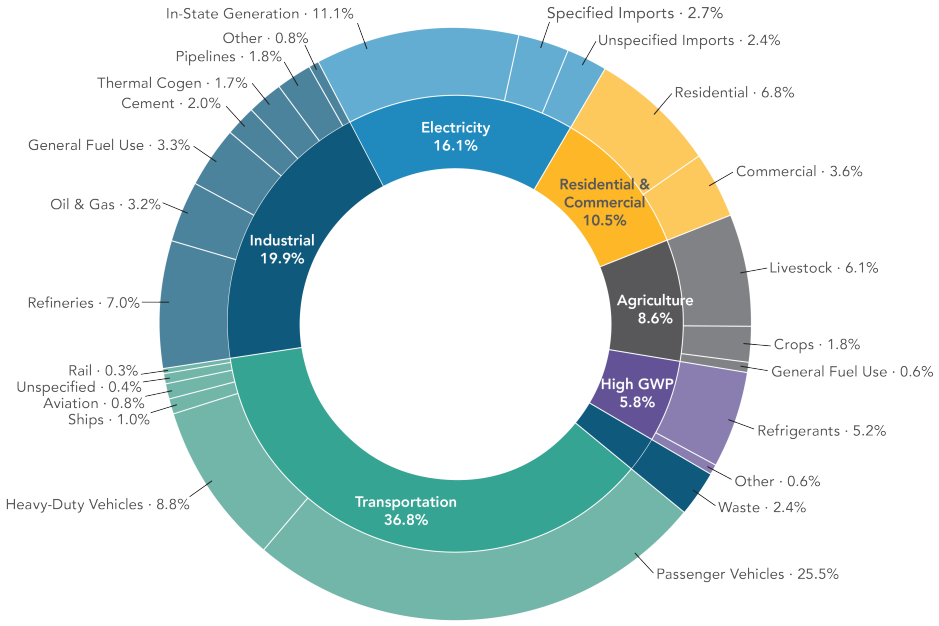

Figure 1.1: Current California GHG emissions inventory data [1]

ufacturer (including total vehicle weight plus fluids, passengers, and cargo). As presented in Figure 1.2, the Federal Highway Administration (FHWA) categorizes vehicles as light-duty LD (Class 1-2), medium-duty MD (Class 3-6), and heavy-duty HD (Class 7-8). EPA also defines vehicle categories by GVWR, but with the purpose of emissions and fuel economy certification [2].

In addition, different types of vehicles can be found in each class as presented in Figure 1.3 which shows typical vehicle types found in the FHWA vehicle classes [3].

As shown in Figure 1.4, MD and HD mobile sources are responsible for 67% of NOx emissions in California, while LD sources account for only 13% of NOx emissions in the state [13]. One reason for this difference is that most HD vehicles are diesel-powered,

Gross Vehicle Weight Rating (lbs)	Federal Highway Administration		US Census Bureau
	Vehicle Class	GVWR Catagory	VIUS Classes
<6,000	Class 1: <6,000 lbs	Light Duty <10,000 lbs	Light Duty <10,000 lbs
10,000	Class 2: 6,001–10,000lbs		
14,000	Class 3: 10,001–14,000 lbs	Medium Duty 10,001–26,000 lbs	Medium Duty 10,001–19,500 lbs
16,000	Class 4: 14,001–16,000 lbs		
19,500	Class 5: 16,001–19,500 lbs		
26,000	Class 6: 19,501–26,000 lbs		Light Heavy Duty: 19,001–26,000 lbs
33,000	Class 7: 26,001–33,000 lbs	Heavy Duty >26,001 lbs	Heavy Duty >26,001 lbs
>33,000	Class 8: >33,001 lbs		

Figure 1.2: Vehicle weight classes and categories from the United States Department of Energy [2].

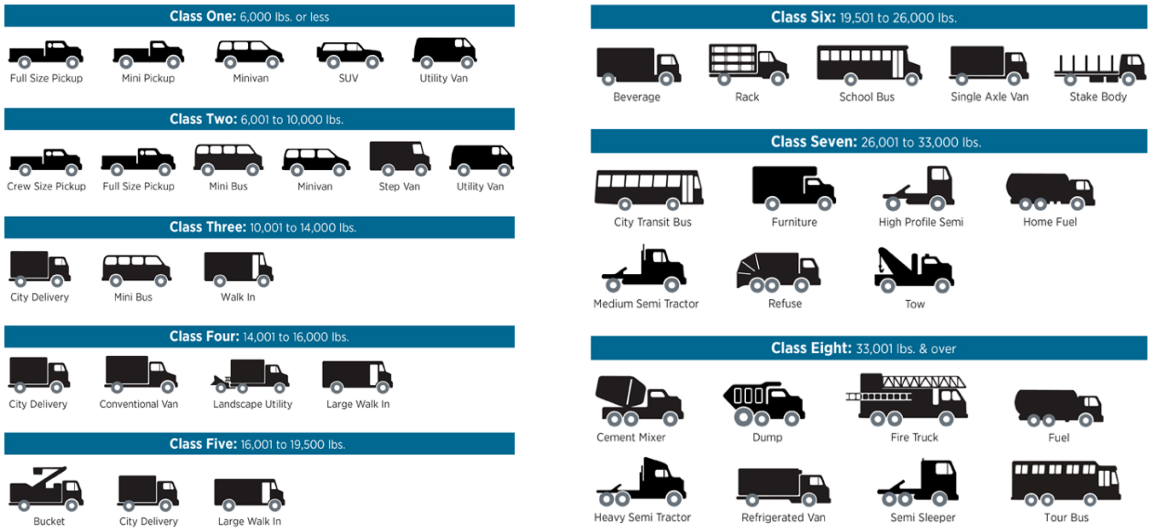

Figure 1.3: Types of vehicles by weight class (one to eight) from the United States Department of Energy [3]

which produce higher NOx emissions per mile than gasoline-powered vehicles. Additionally, HD vehicles travel more miles per year, with an average of 62,229 miles per year, while an average car travels 10,589 miles per year [14].

In recent years, various efforts have been made to reduce emissions from the trans-

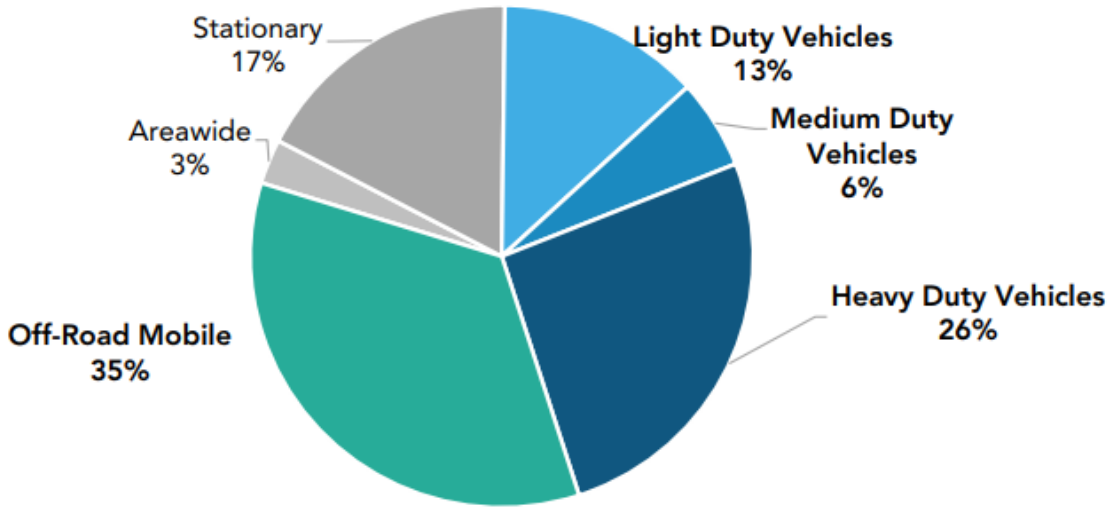

Figure 1.4: NOx emissions in California in 2017 [4]

portation sector, and one of the latest strategies is transportation electrification. According to the 2023 State Transportation Electrification Scorecard from the American Council for an Energy-Efficient Economy (ACEEE), California is the leading state in the US for its actions to support transportation electrification in the LD and HD sectors [15]. The scorecard evaluated different policy developments related to:

- EV charging infrastructure planning and goal setting: government-led planning actions for transportation electrification;
- Incentives for EV deployment: financial and non financial incentives to increase EV purchases and the installation of necessary charging infrastructure;
- Transportation system efficiency: policies that support the deployment of EVs while maximizing emissions reduction;
- Electricity grid optimization: actions taken by public utility commissions to support

utility management; and

- Transportation electrification outcomes: metrics that track progress or evaluate results on EV adoption and infrastructure installation.

Thus, the analysis of California's transportation sector reveals its major impact on greenhouse gas emissions and air pollution, highlighting the variance in emissions across vehicle classes and the state's efforts towards transportation electrification. This sets the stage for a deeper exploration into California's climate goals, emphasizing the urgent need for a transformative approach in the transportation sector and the development of innovative solutions and infrastructure to meet these environmental challenges.

1.1 Motivation

Over the last 50 years, California has made significant progress in air pollution reduction, climate goals, and policy developments. The State has set climate objectives that include a mid-term goal for 2030 to reduce GHG emissions by 40 percent below 1990 levels, as established by Senate Bill 32 [16]. Additionally, there are long-term targets aiming for economy-wide carbon neutrality by 2045 and a reduction of GHG emissions by 80 percent from 1990 levels by 2050, in accordance with Executive Order S-3-05 [17]. This latter target is further emphasized by Governor Brown's Executive Order B-16-2012, which introduces an 80 percent reduction goal specifically for the transportation sector [18]. Moreover, in September 2020, California's Governor issued Executive Order N-79-20, which is a crucial step towards achieving carbon neutrality by 2045 [19]. This Executive Order targets:

- All in-state sales of new passenger cars and trucks to be ZE by 2035;

- All drayage trucks operating in the state to be ZE by 2035;
- All MD and HD vehicles operating in the state to be ZE by 2045, where feasible; and
- All off-road vehicles and equipment to be ZE by 2035, where feasible.

To meet these targets, CARB estimates that approximately eight million EVs and 1.5 million shared chargers will be needed by 2030 to put California on this path [19]. Moreover, CARB estimates that electrifying the state's MD and HD sectors will be critical, and 157,000 chargers will be needed to support 180,000 MD and HD vehicles anticipated for 2030. Additionally, in January 2021, the California Energy Commission (CEC) published a report assessing the EV charging infrastructure needed to support EVs in 2030 [4]. The report highlights several key actions:

1. **Align charging with renewable generation and grid needs:** Pursue greater vehicle-grid integration, as charging millions of vehicles will introduce significant new load onto the grid. Smart charging will help automatically align charging with renewable energy generation, and bidirectional technologies improve resilience and will enable vehicles to supply stored electricity to homes, buildings, other vehicles, or the grid to earn revenue.
2. **Support innovative charging solutions for LD, MD, and HD vehicles:** Explore solutions that can generate new revenue streams, reduce charger costs, improve usage, address the need for grid upgrades, improve resilience, or be uniquely well-suited to specific environments.
3. **Continue modeling efforts to project the quantities, locations, and load**

curves of chargers needed to meet statewide travel demand: Work with partner agencies to incorporate updated electrification and vehicle population scenarios as they become available. Communicate results with load-serving entities and other stakeholders to increase efficacy of infrastructure deployment.

4. **Continue public support for charger deployment, using public funds to leverage private funds, and eventually transition to a self-sustaining private market:** The charging market has introduced diverse and novel business models. The state must continue to invest in charging infrastructure deployment to achieve its ZE vehicle goals. Public investments in charging infrastructure will remain critical to encouraging continued market experimentation, growth, and maturation.

5. **Support local efforts to prepare for transportation electrification:** Recognize that there is no one-size-fits-all charger, and that local conditions will determine the most appropriate solution.

6. **Ensure equitable distribution of charger deployment throughout the state:** Maintain ongoing analyses, such as those called for by Senate Bill 1000, intended to ensure that chargers are equitably and proportionately deployed throughout California.

7. **Prioritize standardized charger connectors and, for networked charging, prioritize hardware capable of standardized communications protocols:** These standards will promote greater driver convenience, interoperability, and grid-integrated charging at the necessary massive scale.

It is critical for California to align EV charging with renewable energy generation, as charging a large number of EVs at the wrong times will introduce a considerable new stress on the electric grid. In fact, a model developed by CEC and the National Renewable Energy Laboratory (NREL) projected that the bulk of EVs charging by 2030 will not align with daytime solar generation and that electricity consumption will add an extra load of 3.6 GW at midnight, when off-peak electricity rates apply and ZEs electricity is not available. The model also flags the importance of TOU rates to shift loads to more favorable times and highlights the crucial need for incentives and other rates strategies to encourage smart charging and vehicle-grid integration [19]. CARB also described the importance of electrification efforts and charging strategies applied to MD and HD fleets, particularly for Class 8 drayage trucks. The ports of Los Angeles and Long Beach (usually called together the San Pedro Bay Ports), are the largest container shipping ports in the US, handling about 40% of the waterborne imported cargo into the nation [20]. Consequently, the California South Coast region and San Joaquin Valley suffer some of the worst air pollution in the nation mostly related to truck activity and drayage operations [4]. Thus, CARB and CEC clearly state that more research and more pilot studies are needed to address these issues. California needs to continue working on EV charging strategies, in particular applied to HD vehicles to meet current climate targets.

1.2 Problem Statement and Contribution of the Dissertation Research

Thus, shaped by California's current statewide goals, this dissertation research focuses on proposing data-driven coordination techniques through intelligent charging and innovative pricing strategies for LD, MD, and HD EVs. The specific contributions of this dissertation can be summarized as:

- Proposing a real-time, data-driven carbon-based pricing model for EV charging that emphasizes times of high renewable energy availability, accounts for local solar PV and building power variations, includes a TOU pricing structure, and employs machine learning (ML) for day-ahead and three-hour-ahead forecasting, with a focus on pattern recognition.

- Identifying trip-and-tour patterns for battery electric trucks (BETs) in drayage operations at San Pedro Bay ports by utilizing data-driven clustering techniques, adjusting energy efficiency for loaded and unloaded conditions, and simulating various charging scenarios to determine SOC, considering potential en-route opportunity charging at specific power levels.

- Proposing an intelligently controlled charging model for BETs to optimize tour completion and reduce charging costs using TOU energy rates. This approach was demonstrated through a one-year analysis of real-world activity data from a fleet operating at the Ports of Los Angeles and Long Beach. The effectiveness of the algorithm was further validated through a sensitivity analysis comparing reserved SOC scenarios of

5%, 50%, and 80%.

1.3 Outline of the Dissertation

This dissertation is organized as follows: Chapter 2 describes the research background of this dissertation and conducts a literature review on several related topics, including EV charging technologies and techniques, pricing strategies, and charging demand applied to BETs. Chapter 3 presents a data-driven dynamic carbon-based pricing strategy and predictions to charge EVs that consider CO_2 emissions from the grid, local solar PV electricity generation, building power usage, TOU rates, and Carbon Allowance Prices (CAP). Chapter 4 introduces an intelligently controlled charging model for BETs to optimize tour completion and reduce charging costs using TOU energy rates. Additionally, a two-stage clustering technique to identify trip-and-tour patterns of BETs, as well as determining if they are loaded or unloaded, is introduced to then simulate their energy consumption and SOC at different locations. Chapter 5 concludes this dissertation by presenting the publications resulting from this dissertation, as well as pointing out some future directions in research. Figure 1.5 presents the general framework of the dissertation.

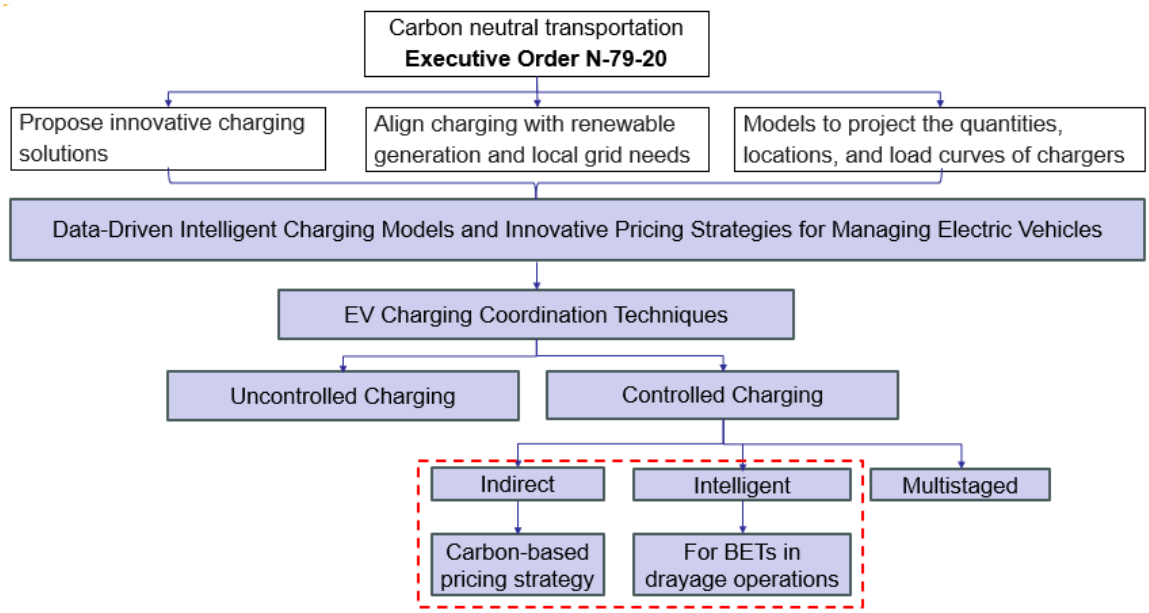

Figure 1.5: General framework of the dissertation.

Chapter 2

Research Background and Literature Review

2.1 Review on EV Charging Technologies

EVs operate with electrical power supplied by an electrical charger usually connected to the power grid. This electrical power from the grid is generated in real-time, affecting the stability of the power grid every time there are fluctuations created by the EV charging loads [5]. As shown in Figure 2.1, there are three charging technologies currently available: conductive charging, inductive charging, and battery swapping.

In conductive charging a physical connection with wires is created so electrons can flow from the charger to the EV battery [21]. This is one of the most mature and commonly used technology for charging EV batteries currently available including HD EVs [5]. The main reasons they dominate the market are its scalability and availability at different power

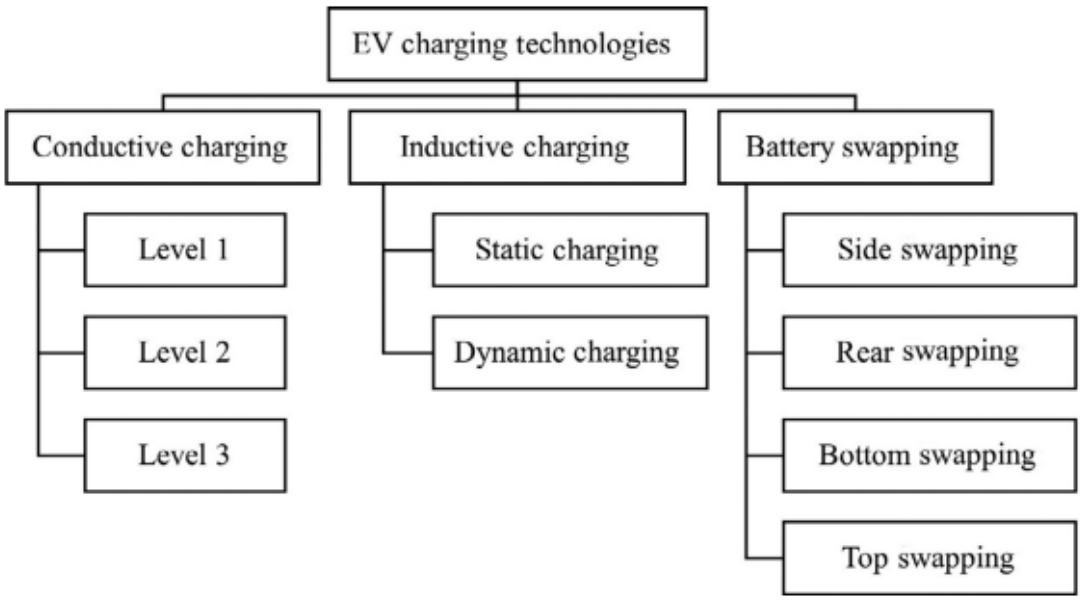

Figure 2.1: EV charging technologies [5]

levels. However, its main limitations are the need for a physical point of contact while the vehicle is stationary, and also the user interaction to plug-in and unplug the vehicle. Level 1 conductive charging represents 120 Volt charging using a common household outlet. This is the slowest method only adding about 3.5 – 6.5 miles of driving range per hour of charging time [22]. Level 2 conductive charging is a 240 Volt charging and one of the most useful and fastest home or public charger technology [23]. However, it requires the installation of a charging station. In addition, depending on the battery type and circuit configuration, Level 2 chargers usually add about 14-35 miles of range per hour of charging time [22]. Finally, direct current (DC) fast charging (informally called Level 3 charging) is the fastest available option and requires a 480 Volt connection. This type of charging is usually too expensive for home use and depending on the battery type and circuit configuration, DC

fast charging can add a maximum of 10 miles of range per minute of charging time [22].

As described in Figure 2.1, another type of EV charging technology is battery swapping which replaces the discharged battery within minutes with a charged battery. Battery swap is one of the least preferred charging technologies mostly because this bring challenges in infrastructure and interchangeability of batteries. The battery can be swapped at the side, rear, bottom, or top part of the vehicle depending upon the manufacturer. Although, battery swapping seems to be a good alternative for HD truck fleets that drive in a limited territory and often return to home base, challenges remain on the large size and lack of standardization of power batteries [24]. However, despite the challenges, some battery swapping stations have been built with robots that quickly replace small modular battery packs in electric cars in just a few minutes [25]. In China, battery swapping has been a great success, and there are even some cars that do not come with a battery, and the owner of the car pays for "battery as a service" [26].

Finally, another type of EV charging technology is called inductive charging or wireless power transfer (WPT). In WPT the energy flows between primary and secondary coils and there is not physical contact with wires. Static inductive charging refers to charging the vehicle while it is parked so both coils can align allowing approximately 100 kW being transferred within an air gap of 125 mm [27]. Dynamic inductive charging refers to charging the vehicle even when the vehicle is moving, which offers flexibility and the opportunity to charge at any time. In fact, dynamic inductive charging has been gaining a lot of attention in recent years with pilot projects implemented at the Korea Advanced Institute for Science and Technology (KAIST), Oak Ridge National Laboratory (ORNL),

and North Carolina State University (NCST). Although WPT is an emerging technology, it is considered a promising solution that solves the plug-in and unplug interaction, and also decreases charging times and battery size [28]. Table 2.1 summarizes systems parameters, including efficiency, of some static and dynamic WPT projects.

Table 2.1: Summary of systems parameters related to WPT projects. Usually the efficiency is higher for static WPT at higher output power levels, and efficiencies are also higher when comparing static vs. dynamic charging systems [7].

Institute	WPT	Power (kW)	Air gap (mm)	Efficiency (%)	Year
Utah State University	static	5	175-265	90[a]	2012
Saitama University	static	3	200	90[b]	2012
University of Auckland	static	1	100	91.3[c]	2015
UM-Dearborn	static	7.7	200	96[b]	2014
	static	6	150	95.3[b]	2015
ETH Zurich	static	5	52	96.5[b]	2015
KAIST	dynamic	3-25	10-200	72-83[a]	2009
ORNL	dynamic	1.5	100	75[b]	2013
NCSU	dynamic	0.3	170	77-82[b]	2014

[a] AC grid to battery pack efficiency

[b] DC input to battery pack efficiency

[c] Coil efficiency

2.2 Review on EV Charging Coordination Techniques

At the moment, one of the main challenges of EVs is how to manage the electrical power supply and demand in real time. This can bring unpredictable imbalances on the grid. As shown in Figure 2.2, there are different EV charging coordination techniques. In uncontrolled charging, the EV receives power immediately from the grid when connected and the user decides when to stop charging. This method is the simplest and fastest for

the user. However, it exposes the grid due to the delay and lack of information of the loads [5]. The grid could be easily overloaded and the power quality degraded. Another type of EV charging is called controlled charging. This method gathers vehicle charging needs and coordinates charging stations and grid operators to optimize charging and to avoid potential imbalances on the grid. The main three categories of controlled charging are: indirect controlled charging, intelligent controlled charging, and multistaged controlled charging.

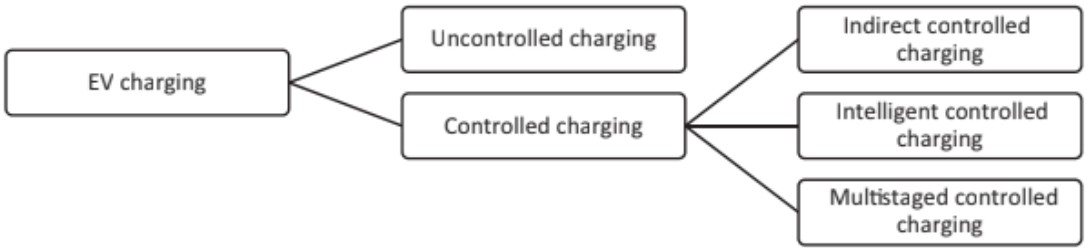

Figure 2.2: EV charging coordination techniques [5].

Indirect controlled charging considers user behaviour to control the parameters that influence the charging method. This can be classified into two categories: spatial load shifting and temporal load shifting. In spatial load shifting financial incentives are used to encourage drivers to use less congested charging stations to distribute the load. Temporal load shifting encourage users to charge during off-peak hours reducing the cost of electricity. Intelligent controlled charging optimizes the resources (such as charging energy cost, or efficiency) based on constraints (such as grid energy demand, battery capacity, network structure, or efficiency of transformers) using a data-driven approach. This method considers EV data, charging stations, user needs, and information from distribution systems

operators. Finally, multistaged controlled charging, also called multistaged hierarchical controlled charging method, is a priority based decision making method. This method usually considers capacity of the infrastructure, priorities of EVs, SOC, charging cost, and TOU to provide an unique solution using a decision based control through a genetic algorithm or artificial intelligence based controls [5]. Multistaged controlled charging also includes bidirectional power flow, also called vehicle to grid (V2G) enabling technologies, to inject power to the grid at times that is needed, usually peak times.

2.3 Review on Indirect Controlled Charging Strategies

Research focused on EV charging techniques and their CO_2 emissions has been growing over the years. There are also several studies targeting solar charging strategies and its impact on emissions, grid balancing [29], policy [30], and pricing behavior. Methodologies for EV charging have changed over time. In 2009, an extensive literature review on EVs and their environmental impacts in Europe mentioned that users could be incentivized to charge EVs during off-peak (night) rather than peak (day time) hours to take advantage of excess baseload capacity during off-peak periods and help balancing grid load [31]. The document also warns about using average CO_2 emission rates to assess emissions associated with EV charging mentioning that this neglects temporal and spatial variations of the energy supply and its implications in the electricity market [31]. Table 2.2 and 2.3 summarize relevant recent publications. The list is extensive, and each work addresses different areas. McLaren et al. from NREL modeled hourly emissions impacts and EVs charging scenarios for five different electricity grid mixes [32]. Similar research related to CO_2 emissions from

EVs is presented in references [33, 34, 35, 36, 37]. Additionally, references [38] and [39] not only studied CO_2 emissions from EVs, but also compare them to internal combustion engines vehicles. Previous work in the area of EVs charging is substantial as presented in references [40, 41, 42, 43, 44, 45, 46, 47] and some of them consider EVs charging integrated with solar PV [48, 49] and wind energy [50]. However, there are still gaps in the collective knowledge, especially in the area of EV pricing strategies. For instance, at most private charging stations (e.g.,ChargePoint) the EV charging rates, access, and policies are set entirely by the charger owner [51]. Thus, EV charging rates vary by station, provider, and operational state. Most charging stations charge a fee while others are completely free of charge. For example, Level 2 ChargePoint station located at the City of Riverside charges $4.99 for 2 hours, while UCR Lot 24 ChargePoint station charges $1.75 per hour for the first 2 hours [52]. Electrify America also provides Level 2 charging at a cost of $0.03 per minute or $0.43 per kWh depending on the location and membership subscription [53]. Although there are regulations for measuring and tolerance in EV charging stations, regulation for pricing does not exists. As a matter of fact, in December 2019, the California Division of Measurement Standards (DMS) finalized the rules for measuring and meter tolerance in EV supply equipment such as EV charging stations. Some of the rules from DMS require the stations to display voltage rating, type of current, maximum power, and the quantity of electricity delivered just to name a few. However, in terms of pricing, the only requirement for the charging station is to clearly display the pricing (easily understood), and also clearly outline between kWh charges, session charges and parking fees [54]. Some authors in academia have proposed pricing strategies considering price stimulus based on

queue, TOU rates, peak power charge, and valley-filling [55, 56, 57]. The response of EV drivers to dynamic pricing focusing on their willingness to pay has also been studied in [58], and [59] proposes a carbon-oriented charging scheme comparing day and night charging. Finally, [60] proposes a pricing strategy applied to fast charging stations considering voltage control. However, none of the works previously mentioned propose a carbon-based pricing that considers in real time the dynamic generation of CO_2 emissions from the grid.

2.4 Review of Intelligent Controlled Charging for BETs

In recent years, there have been multiple efforts to understand truck activity, grid impacts, and charging models for drayage fleets, especially as drayage truck fleets are anticipated to become more electrified and connected in the future [61]. Drayage trucks, which transport cargo containers between ports and nearby distribution centers daily, are considered an ideal candidate for electrification due to their predictable activity patterns. Drayage trucks travel a limited distance each day, typically shorter than the driving range of current BET technologies. They usually return to their home base every night, allowing for overnight charging. Opportunity charging refers to any chance an EV has to charge its battery, including brief stops such as at traffic intersections or while loading or unloading passengers at a bus station for instance [62, 7]. Moreover, several studies have targeted zero-emission drayage operations in Southern California. In 2012, a report prepared from Gladstein for the South Coast Air Quality Management District (SCAQMD) highlighted the potential benefits of catenary-accessible hybrid trucks at the port of Los Angeles [63].

Table 2.2: Summary of indirect controlled charging related work

Ref.	Short summary
[33]	Emissions associated with plug-in EVs and their impact on the grid and cost
[38]	CO_2 emissions comparison between EVs and conventional cars
[29]	Grid balancing with wind power and EV charging
[30]	Assessment of EVs on peak and off-peak charging policies
[34]	CO_2 emissions from EVs charging (a case study)
[35]	CO_2 emissions optimization on plug-in hybrid EVs
[36]	CO_2 emissions from EVs charging in 2030 using an optimizing energy system model
[37]	CO_2 emissions from EVs charging in Rome
[32]	CO_2 emissions from EVs and plug-in hybrid vehicles charging under five carbon intensity grid scenarios
[39]	Comparison of EVs and internal combustion engines vehicles global warming potential in European countries
[40]	EVs charging behavior scenarios in a smart grid
[58]	EV drivers response to dynamic pricing (willingness to pay)
[41]	EV charging using a behavioral model and a electricity system
[60]	EV fast charging pricing strategy for voltage control
[42]	Predictions of EV charging demand based on scenarios
[43]	EV charging methods considering peak load and voltage violation
[48]	Photovoltaics (PV) based EV charging considering state of charge (case study)
[44]	Dynamic EV charging and its effect on imports and exports of energy
[55]	EV charging strategy considering price stimulus and the queue of EV fast charging station
[45]	EV charging scheduling considering valley filling and scenario based approach
[59]	Day and night CO_2 emissions comparison from EVs charging sessions
[49]	EV coordinated charging with solar PV while minimizing probability of voltage and current noncompliance (case study)
[57]	EV charging pricing strategy considering TOU, valley-filling, and peak-shifting
[46]	EV charge scheduling considering valley-filling, and improving Solar PV error forecast using sky imager (case study)

Table 2.3: Summary of indirect controlled charging related work (cont.)

Ref.	Short summary
[56]	EV charging pricing per session considering TOU and peak power charge
[50]	EV charging to minimize CO_2 emissions and optimize wind energy usage
[47]	EV charging, automation, and sharing considering load patterns, peak power, battery capacity, renewable curtailment, and GHG emissions.

Developments moved forward, and in 2017 Siemens built a test "eHighway" in Carson, California, near the port of Long Beach. The system only had three freight trucks that can pair with the one mile long catenary system: a BET, a natural gas hybrid-electric truck, and a diesel-hybrid truck. The trucks were ZEs when connected to the catenary, and when the eHighway ended, the trucks returned to use their internal engine to drive the rest of the path [64]. In addition, in 2013, a report from CALSTART aimed to research, identify, and evaluate potential technologies to address drayage needs while achieving ZEs in the San Pedro Bay Ports [65]. This report was intended to specify the requirements that zero-emission trucks must meet in order to substitute conventional diesel trucks, emphasizing the importance of routing strategies to improve productivity [65]. Numerous studies have explored the activity patterns of drayage operations. In [66] truck trips were analyzed, finding that less than 1% of drayage trucks completed more than 5 trips per shift, and on average a truck delivered 12 round trips per day. The paper also mentions that the trucks spend most of its time navigating to the port and dealing with cargo logistics (port access, loading, etc.), completing about 60 miles per day near-dock service [66]. In a separate study, Tanvir et al. [67] analyzed the activity of drayage trucks in Southern California to estimate the corresponding electric energy consumption and SOC of their batteries.

Their results suggest that BETs can serve 85% of the tours if they can be opportunity charged at the home base between consecutive tours. In addition, drayage fleet efficiency has also been studied. In [68], a drayage operation planning approach that minimizes cost and maximizes productivity was presented to deal with port access restrictions by slot capacity availability. Their results showed that drayage activity productivity can be increased by 10-24% when port access capacity is increased by 30% [68]. Furthermore, drayage truck emissions have also been assessed over the years. In [69], a coordinated truck model was presented to reduce emissions from empty truck trips. Their results suggest that a collaborative truck appointment system is an effective tool to reduce emissions, but that a congestion management tool is also needed at ports [69]. McCormack et al. [70] measured truck movements along specific roadway corridors in Washington State using data from the Commercial Vehicle Information System and Networks (CVISN) electronic truck transponders and Global Positioning System (GPS) data from 30,000 trucks. Results showed that GPS devices provided highly accurate data on both travel routes and individual roadway segments used by trucks. This makes the GPS dataset considerably more robust than the transponder data. Ma et al. [71] analyzed GPS truck data to develop performance measures for truck-based freight network monitoring. Truck travel patterns were identified using an algorithm that differentiated between traffic-based stops and intended stops. This algorithm utilized average stop duration (i.e., dwell time), and the results were manually inspected. The findings presented travel time and speed, roadway location, and stop location information for a fleet of 2,500 trucks in the Puget Sound, Washington region.

You et al. [72] developed a comprehensive framework for processing GPS data from

clean trucks at California's San Pedro Bay Ports. Data from 545 trucks were filtered and manually checked for truck-accessible locations using Google Earth. Four tour type patterns were analyzed, concluding that the tour characteristics of trucks vary significantly based on fuel type and cargo moves. Similarly, Patel et al. [73] utilized a Random Forest classifier to categorize truck stop locations as either primary or secondary using GPS data. Their proposed machine learning model can identify primary stop locations with an accuracy of 97%.

Zhu et al. [74] conducted a systematic study on the impact of charging loads of HD EVs on the electric power grid. They used a methodology that takes into account the location of chargers, load modeling, and grid impact analysis, and compared the results using one model distribution feeder and a realistic California feeder. The study revealed the impact of charging stations on the grid and suggested that different mitigation plans, such as the use of smart chargers, can provide reactive power support. Fjaer et al. [75] modeled the aggregated load profiles of high-energy charging stations utilized by HD EVs in Eastern Norway, considering peak loads of 4, 9, and 13 MW. The findings showed that the peak loads associated with HD EVs caused the electrical distribution substation to surpass its rated capacity and thermal limit. To address this issue, the authors suggested reducing the peak load by extending the drivers' break time by 15 minutes, which would enable the operation of the electrical distribution substation to remain below the rated capacity. This recommendation aimed to ensure that the substation operates within its limit and provides a stable power supply.

Borlaug et al. [76] investigated the impacts of depot charging by developing syn-

thetic load profiles for short-haul HD EVs, which were applied to 36 distribution substations. The results showed that 78-86% of the substations were capable of supplying HD charging without upgrades. In [77], a simulation was conducted to assess the impact of HD charging on a distribution system in Texas. The findings indicated that the transmission grid experienced a significant impact when charging only 11% of the simulated HD EVs, highlighting the need for infrastructure upgrades and further studies of smart charging models. Similarly, Tong et al. [78] analyzed the charging load profiles of HD EVs, which demonstrated that the daily charging peak is highly influenced by long-haul truck operations, as well as the peaks in solar power generation in California. Smart charging for HD EVs, explored in [79], used data from 259 U.S. HD EVs to gauge peak demand impacts. Modeling two battery capacities and charging levels, the findings showed that smart charging could reduce peak demand by 1,095 kW, potentially saving up to $10,000 monthly.

The review of these prior research efforts suggests significant gaps in the existing literature concerning in depth analysis of drayage truck operation, stop locations, and energy consumption. Moreover, while the estimation of grid impacts from HD truck charging has been explored, it has not been specifically examined for drayage operations. Lastly, the development of intelligent charging models tailored for HD trucks is almost non-existent to date. While there are various factors that affect the performance of BETs, including temperature conditions, battery degradation, and battery cell imbalance, literature is limited [80, 81] as electric trucks are greatly influenced by technological advancements. Consequently, given the rapid progress in battery technology, the feasibility of HD BETs is changing rapidly [82].

Chapter 3

Indirect Controlled Charging Through a Carbon-Based Pricing Strategy

Transitioning from basic concepts and policy discussions about California's transportation sector, this section introduces methods and data analysis centered on a detailed approach to controlled electric vehicle charging, influenced by carbon pricing strategies. It serves as a key point in the dissertation, where theoretical ideas are put into practice through thorough research methods, aiming to tackle the challenges of transportation electrification with a focus on inventive and environmentally-aware charging solutions. Figure 3.1 presents the framework of this chapter.

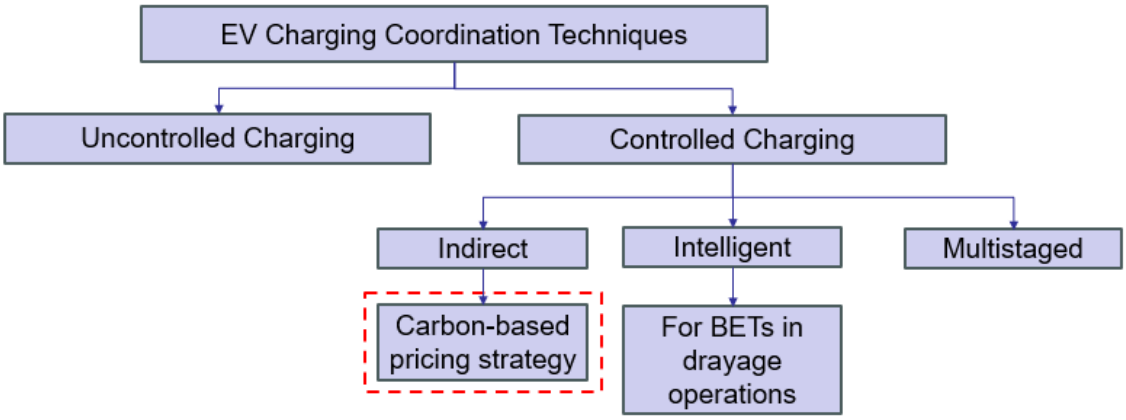

Figure 3.1: Framework of this chapter.

3.1 Introduction and Background

In order to achieve carbon neutrality by 2045, it is estimated that California will need approximately eight million EVs and 1.5 million shared chargers by 2030 [19]. It is clear that innovative charging solutions will be needed to align EVs charging with renewable energy generation and local grid needs. Over the years, there has been numerous research studies focused on CO_2 emissions associated with EV charging, solar charging strategies and its impact on emissions, grid balancing, policy, and pricing behavior. In order to avoid loads on the grid at unfavorable times, it is imperative to align EVs charging with renewable energy generation, to seek strategies to encourage smart charging, and to ensure consistency in EVs charging pricing.

3.2 Chapter Problem Statement

What is needed is a method to ensure consistency in EVs charging pricing, align EVs charging with renewable energy production, and consider the local needs of EV users. In this chapter, an Intelligent Transportation System (ITS) approach was developed to optimize EV charging based on constraints of the electricity grid. Specifically:

- We developed a data-driven dynamic carbon-based pricing strategy to encourage EV charging during times of the day where an excess of renewable energy occurs;
- We considered the local needs by adapting the pricing model to include building loads and clean solar PV energy generation–the pricing model is able to capture the variability of solar PV power and building power usage and adapts in real-time to current conditions;
- We introduced a TOU pricing mechanism as an addition to the carbon-based pricing strategy to incentivize drivers; and
- We generated carbon pricing day-ahead and three hour-ahead predictions using ML to help drivers better plan their charging sessions accordingly. This innovative EV pricing methodology is based on pattern recognition through ML rather that simple simulated scenarios.

3.3 Methodology

3.3.1 Proposed Pricing Strategy

In order to propose a carbon-based pricing strategy in \$/kWh to charge EVs, data from the California Independent System Operator (CAISO) and CE-CERT was gathered. The main goal was to combine the information from the energy grid (CAISO) and a university-operated microgrid to optimize the hours when EV charging is favorable. To assess the CO_2 emissions from EVs, the CO_2 emissions rate from the grid is used. This rate represents the CO_2 emitted to generate one MWh of electricity and is calculated by dividing the CO_2 emissions ($mTCO_2/h$) by the total energy supply from the grid (MW). Subsequently, this rate ($mTCO_2/MWh$) will be complemented by adding Carbon Allowance Prices (CAP) in \$/$mTCO_2$ and TOU in \$/kWh. This methodology is illustrated in Figure 3.2.

CE-CERT's microgrid generates its own electricity from solar PV during the day, and the surplus is being exported to the grid. So, the energy being used during solar production hours is carbon-free. Thus, our model calculates and predicts the carbon-based EV charging pricing scheme at each timestamp i as follows:

$$\frac{\$}{kWh_i} = \left[\Big(\underbrace{\frac{mTCO_2}{kWh}_i \times WF_i}_{\text{Grid}} \times \underbrace{\frac{\$}{mTCO_{2\,i}}}_{\text{CAP}} \Big) + \underbrace{\frac{\$}{kWh_i}}_{\text{TOU}} \right] \times \underbrace{(1 - f_{solar})_i}_{\text{CE-CERT}} \tag{3.1}$$

Where:

$mTCO_2/kWh$ = CO_2 emissions rate from the grid for all energy sources combined.

WF= Weighting factor defined as the ratio of energy supply by source to the total energy

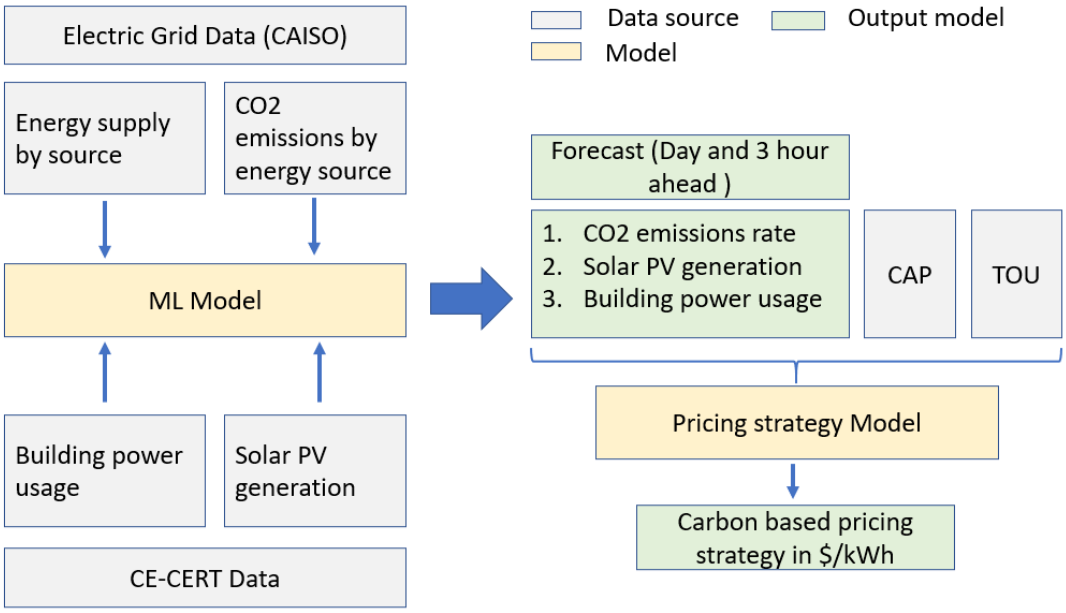

Figure 3.2: Proposed carbon-based pricing methodology. Grey boxes correspond to data sources, yellow boxes correspond to models created, and green boxes correspond to model output.

supply. This factor is being applied to capture the increase and decrease in energy supply and emissions from each source (e.g.,in order to capture the decrease in energy supply from natural gas during solar generation we need to weight the supply from natural gas with respect to the total supply).

CAP = Carbon Allowance Prices. These allowances are created by CARB based on the total number of permissible emissions. One allowance equals one metric ton of carbon dioxide equivalent emissions [83]. The number of allowances created is reduced every year, so the annual CAP declines. CAP prices are set each year in February, May, August and November by CARB [83]. Joint Auction #25 held in November 2020 set the carbon allowance price that run from November 17 2020 to February 17 2021 to 16.93 \$/mTCO$_2$ [83, 84].

TOU = Riverside Public Utilities (RPU) TOU for Large and general industrial services [85,

86]. They define their electricity prices in $/kWh and their Summer electricity rate starts at 12:00 am on June 1^{st} and continue through September 30^{th} of each year. Winter electricity rate starts at 12:00 am on October 1 of each year and continue through May 31 of the following year [86]. Table 3.1 summarizes RPU-TOU.

Table 3.1: 2020 RPU TOU

Energy Charge	Description	$\$/kWh$
On-Peak	12:00pm-6:00pm summer weekdays 5:00pm-9:00pm winter weekdays except holidays	0.1079
Mid-Peak	8:00am-12:00pm summer weekdays 6:00pm-11:00pm summer weekdays 8:00am-5:00pm winter weekdays except holidays	0.0874
Off-Peak	All other hours	0.0755

f_{solar}= Solar factor. This factor can take values between 1 and 0 and considers solar PV power and building power usage. This is calculated as follows:

$$f_{solar} = \frac{Solar\ Power\ (kW)}{Building\ Power\ Usage\ (kW)\ +\ Solar\ Power\ (kW)} \tag{3.2}$$

So

$$f_{solar} = \begin{cases} 1 & \text{Building Power Usage} \leq 0 \\ [0, 1[& \text{Otherwise} \end{cases} \tag{3.3}$$

When f_{solar} is 1, this means that the building is being supplied entirely by solar energy and the surplus is exported to the grid, so $(1 - f_{solar})$ would be zero, and therefore, there would zero CO_2 emissions from the grid during this time. Finally, by using Equation 3.1, we can get a carbon-based pricing scheme in $/kWh that considers the emissions associated with the source of electricity used by the EVs, carbon allowance prices, TOU, and PV generation

at CE-CERT. For our model, we make the following assumptions:

1. The goal is to generate predictions in real time. However, to present this work, we are assuming November 21^{st} 2020 as our target day for day-ahead prediction. This means that the day-ahead model has been tested and trained using data up to 23:59pm of November 20^{th}.

2. We also assume November 21^{st} 2020 at 09:45am is our target day and hour for the three hour-ahead prediction. This means that the three hours ahead has been tested and trained using data up to 09:45am of November 21^{st}.

3. We assume that the grid coming in to CE-CERT has the same energy source composition as the grid data from CAISO.

3.3.2 Data

3.3.2.1 CAISO Data

Real-time energy supply by source data and real-time CO_2 emissions by source data were collected from CAISO. Data were collected every 5 minutes from April 2018 to November 2020. The energy supply by source data is collected in MW and the CO_2 emissions by source is collected in $mTCO_2/h$. CO_2 emissions from CAISO are calculated by adding GHG emissions from internal ISO dispatches, including dynamic schedules, and GHG emissions from imports serving ISO load [87]. Figure 3.3 shows CAISO energy supply by source for November 20th 2020. Figure 3.4 shows grid CO_2 emissions by source in $mTCO_2/h$ for November 20th 2020. A decrease in energy supply and emissions from imports

and natural gas is observed when solar energy supply increases, which for this particular day, happens around 8:30am.

Figure 3.5 shows CO_2 emissions rate from the grid multiplied by each weighting factor in $mTCO_2/MWh$. This corresponds to the first horizontal bracket in Equation 3.1. Natural gas usage and imports supply started to decrease as soon as solar energy was being generated. Usually, imports and natural gas supply will remain at their minimum during solar generation hours. However, this may not be the case when we have a cloudy day, or if it is a particularly hot day and the energy demand increases due to the air conditioning (AC) usage.

3.3.2.2 CE-CERT Data

The CE-CERT buildings are connected to the grid and also generate electricity from 500 kW of installed PV solar arrays. Typical loads of the CE-CERT buildings include level-3 EV charging, level-2 EV charging, heating ventilation and air conditioning (HVAC) operation, lightning and other operational loads. Real-time building power usage data, which corresponds to the readings from the meter, are collected every thirty seconds, and real-time PV generation data are collected every 15 minutes. Both are collected in kW. Building power usage and PV generation data were collected from January 2017 to December 2020 and are divided into Fall, Winter, Spring, and Summer quarters to generate seasonal predictions. Figure 3.6 shows the typical building power usage and solar PV generation at the CE-CERT facility in kW. On a normal sunny day, building power usage is negative during solar PV generation. This means that the energy usage of the building is

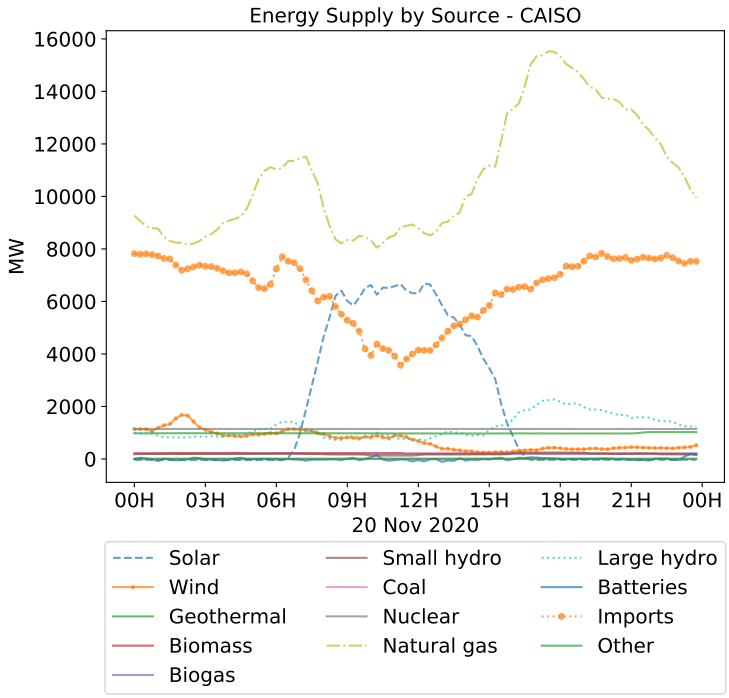

Figure 3.3: CAISO grid energy supply by source in MW for November 20th 2020.

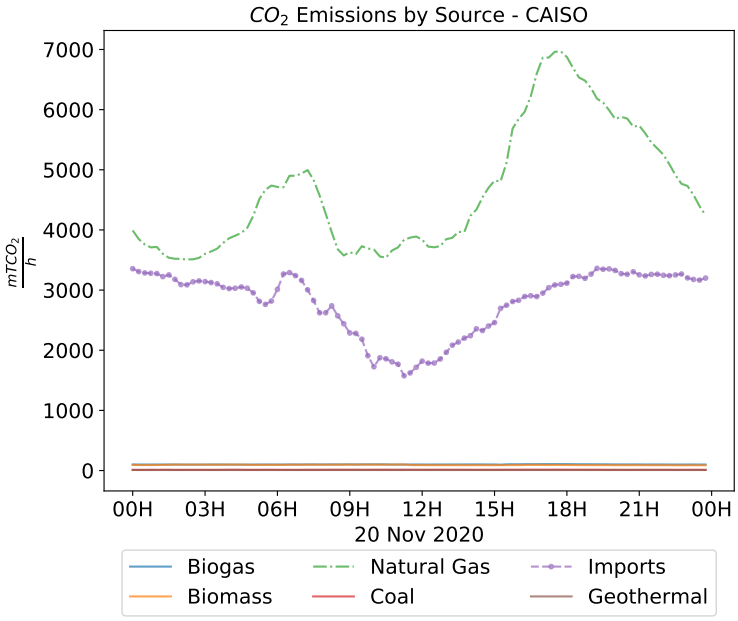

Figure 3.4: CAISO grid CO_2 emissions by source in $mTCO_2/h$ for November 20th 2020.

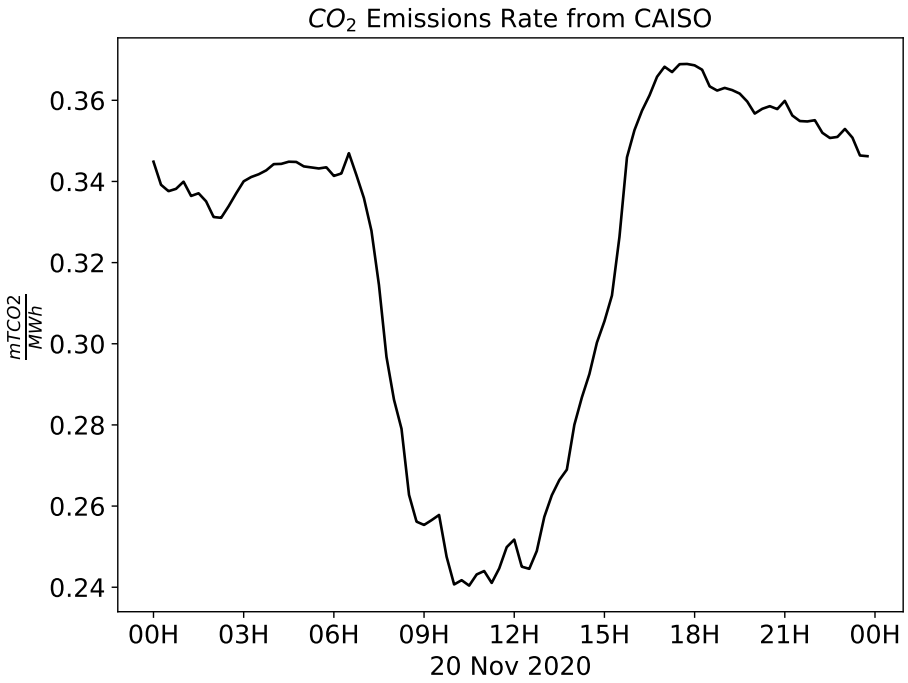

Figure 3.5: Weighted CO_2 emissions rate in $mTCO_2/MWh$ for November 20th 2020.

supplied entirely by solar generation and the surplus energy is being exported to the grid. Figure 3.6 also illustrates the values of f_{solar}, which is equal to one at times when energy is exported to the grid, as described in Equation 3.3.

3.3.3 Forecast using ML

Predictions of CO_2 emissions rates from the grid, solar PV power, and building power usage from CE-CERT were generated by using a supervised ML regression model called Random Forest regression in Python [88].

Random Forest regression is a supervised machine learning model designed to learn by training. The decision trees are built in parallel during training and the output

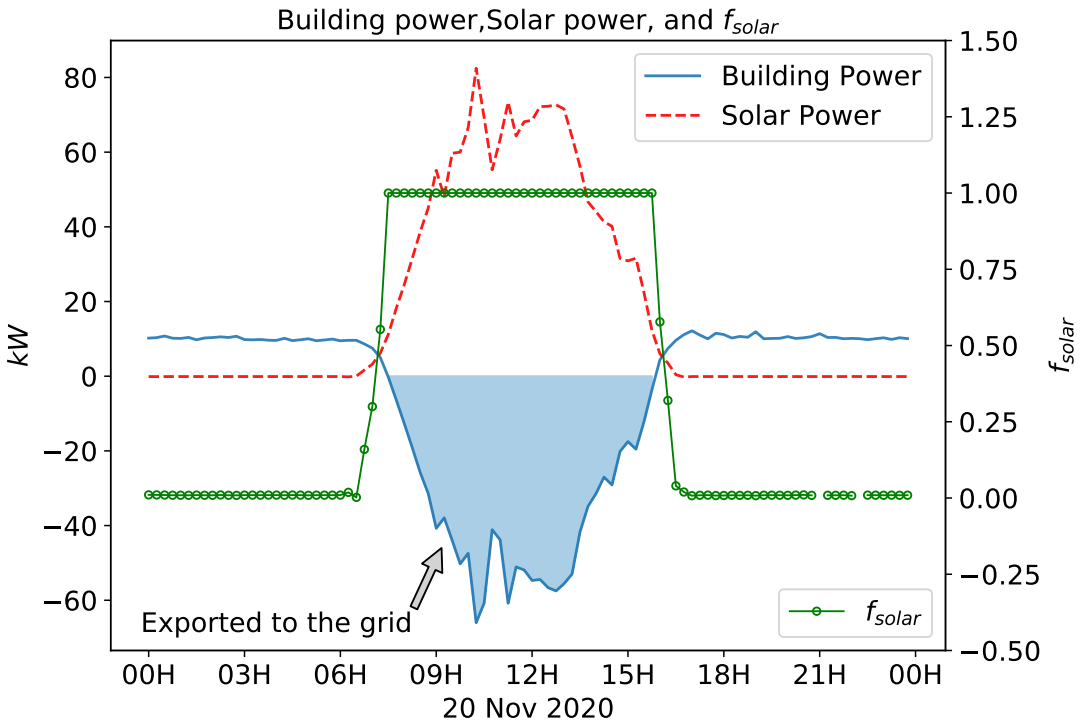

Figure 3.6: Building power usage, solar PV generated, and f_{solar} at CE-CERT for November 20th 2020. This particular building is connected to 100 kW of installed PV solar arrays.

result is the mean of all the prediction trees [88]. Random Forest was chosen based on previous work from [89] where different machine learning models are used to predict solar PV power, showing that Random Forest had the best overall performance. Our model is highly dominated by solar PV power production, so we assume that this model would fit well with our datasets. In addition, Random Forest is one of the most accurate learning algorithms available and runs efficiently on large databases [88]. However, special attention is needed to avoid overfitting. This can be controlled by running a cross-validation process that utilizes different settings to evaluate the performance of the estimator [90].

For our machine learning model, we used a train-test split ratio of 70-30%. We ran a cross-validation using 5 folds with 3000 fits to validate our model. Finally, the Root

Mean Square Error (RMSE) and coefficient of determination (R^2) were used to evaluate the final performance of our model.

3.4 Results and Discussion

3.4.1 CO_2 Emissions Rate Forecast

The first term in Equation 3.1 represents the CO_2 emissions rate from the grid. The output of the forecast model is day-ahead and three-hour-ahead CO_2 emissions rate predictions. When running the cross-validation with a total of 3000 fits, the best performance was achieved with 950 and 970 estimators (number of trees in the forest) for day-ahead and three-hour-ahead predictions respectively. Figure 3.7 illustrates a few combinations of the day-ahead cross-validation. When running the model with the following parameters settings: maximum features (number of features to consider at every split)=*auto*, minimum samples leaf (minimum number of samples required at each leaf node)=*1*, and random state=*42*, we achieved a better mean R^2 and RMSE overall than when we changed to minimum samples leaf=*2*. Negative RMSE sign represents loss, so the magnitude was considered.

Figure 3.8 shows the result of the day-ahead (DA) and three-hour-ahead (3 HA) CO_2 emissions rate forecast for November 21^{st} 2020. The day-ahead prediction follows the correct trend. Moreover, the three-hour-ahead prediction was able to adapt to the sudden change of the trend by updating the prediction from 0.15 to 0.20 $mTCO_2/MWh$ around Noon.

Table 3.2 summarizes the error metrics for the day-ahead and three-hour-ahead

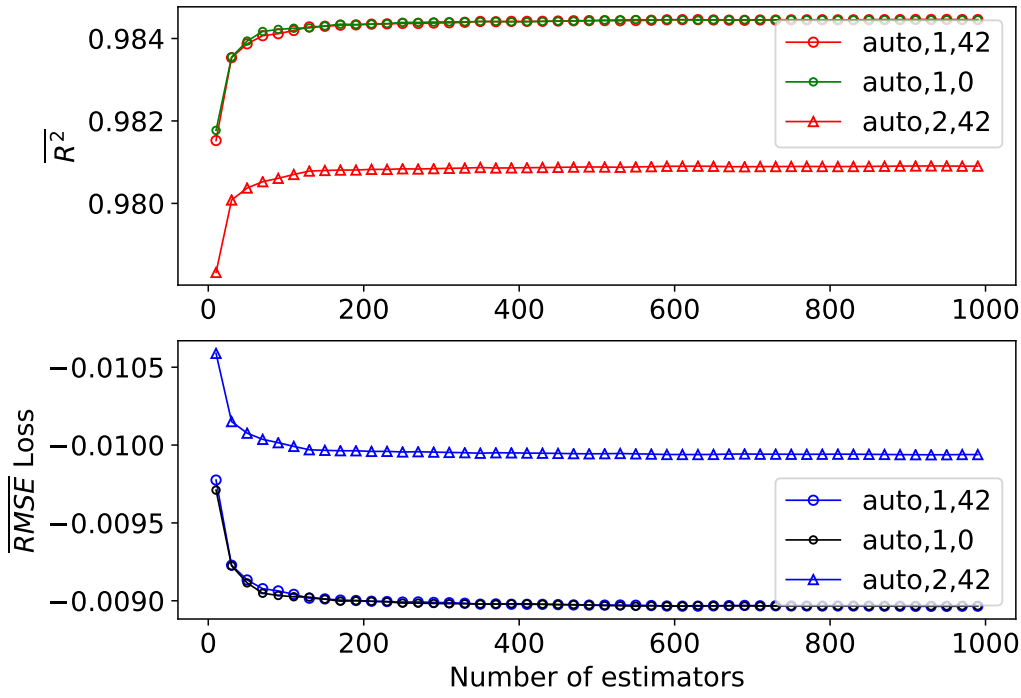

Figure 3.7: Result of cross-validation to get the best combination of hyperparameters for predicting CO_2 emissions rate in $mTCO_2/MWh$. Number of estimators corresponds to the number of trees in the forest, and maximum features=*auto* means $\sqrt{number\ of\ features}$.

CO_2 emissions rate predictions. Overall, the day-ahead prediction performs better than the three hour-ahead predictions. This is due to the number of estimators and random state of the model for each prediction. Overall, for day-ahead prediction, the model has a RMSE of 0.0083 $mTCO_2/MWh$ which is relatively small when compared to the magnitude of the CO_2 emissions rate.

3.4.2 Solar PV and Building Power Usage Forecast

The fourth term in Equation 3.1 considers the contribution of solar energy generated compared to building power usage at CE-CERT by using the solar factor (f_{solar}). The best performance of the day-ahead solar PV power predictions was achieved with 950

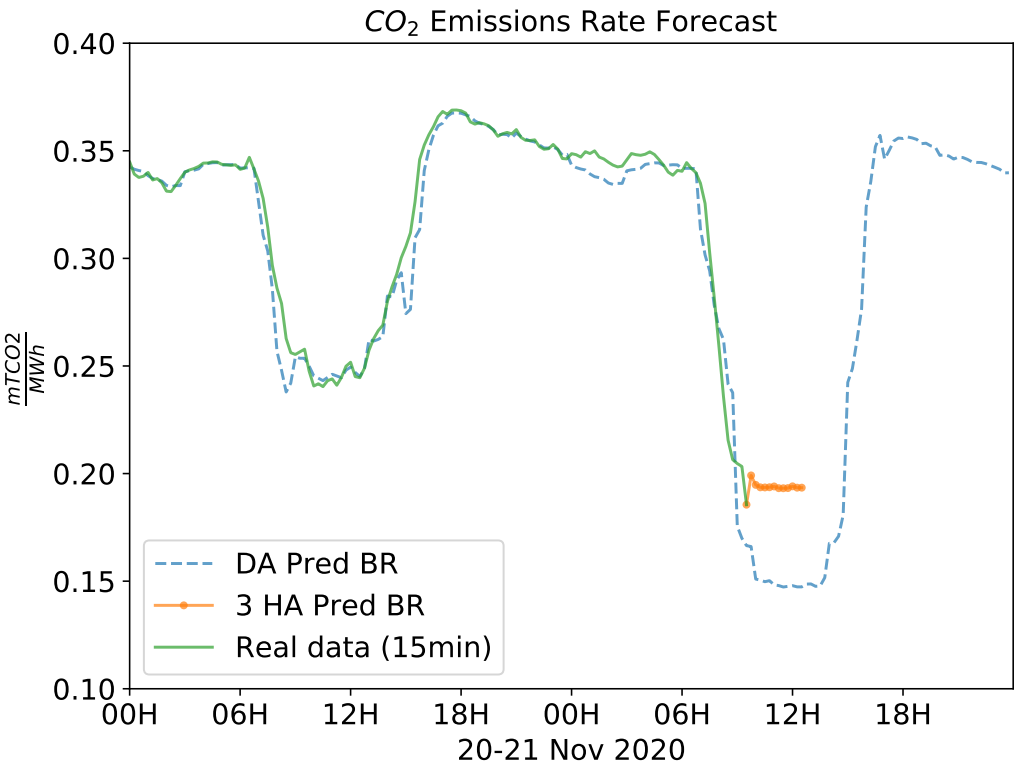

Figure 3.8: Day-ahead (dashed blue line) and three-hour-ahead (dotted orange line) CO_2 emissions rate forecast for November 21 2020. "BR" means best Random Forest model which includes the results of the cross-validation.

estimators and 990 estimators for three-hour-ahead predictions for Fall (because November 21st is in the Fall quarter).

Table 3.2 summarizes error metrics for day-ahead and three-hour-ahead solar PV power predictions. Having an overall RMSE of about 6 kW for day-ahead predictions is acceptable when solar PV power ranges from 0 to 80 kW. Figure 3.9 shows day-ahead and three-hour-ahead solar PV power forecast. It also shows $y - \hat{y}/\sigma$ which is presented as an error metric to illustrate that even with sudden changes in solar PV power due to clouds or other factors, the error is still within a small range.

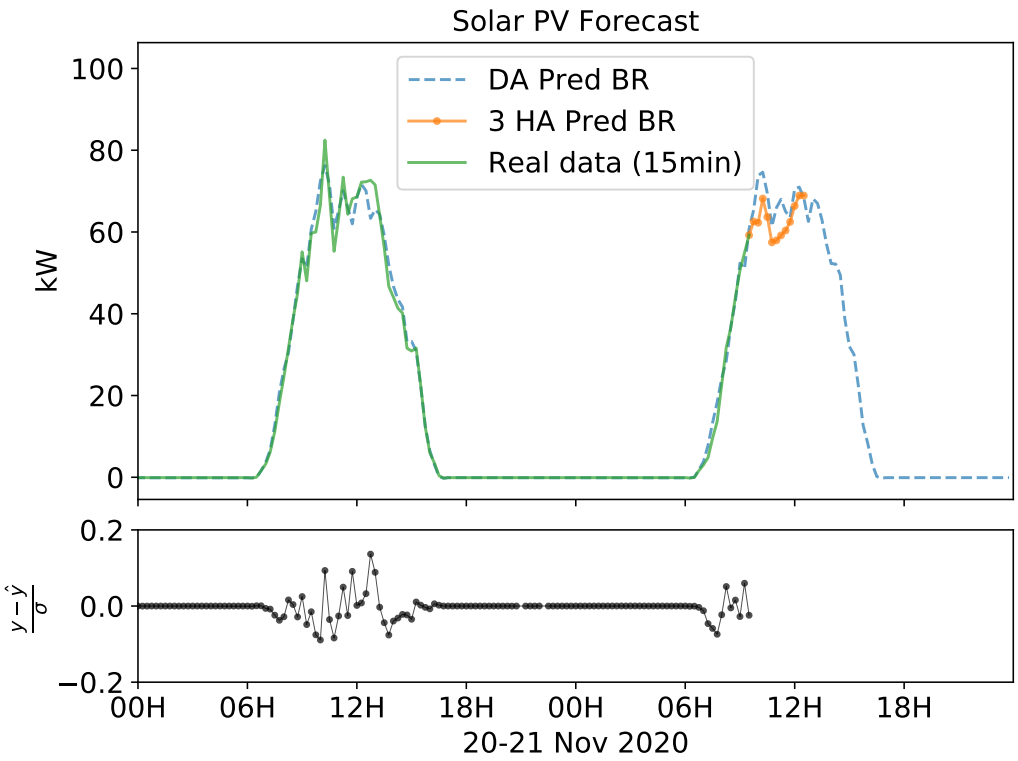

Figure 3.9: Solar PV power forecast. Day-ahead (dashed blue line) and three-hour-ahead (dotted orange line) for November 21 2020. "BR" means best Random Forest model which includes the results of the cross-validation.

In order to calculate f_{solar} (Equation 3.3) building power usage also needs to be predicted. The best performance of the day-ahead building power usage predictions was achieved with 970 estimators and 870 estimators for three-hour-ahead predictions for Fall. Figure 3.10 shows day-ahead and three-hour-ahead building power usage forecast.

Similarly, building power usage error metrics are presented in Table 3.2. Although building power usage is strongly dominated by solar PV, the prediction presents a lower performance when compared to solar PV power forecast. This may be caused by the granularity of the data. Building power usage data were collected every 30 seconds and averaged to 15 minutes for consistency and GPU resources. As a result, the model may not

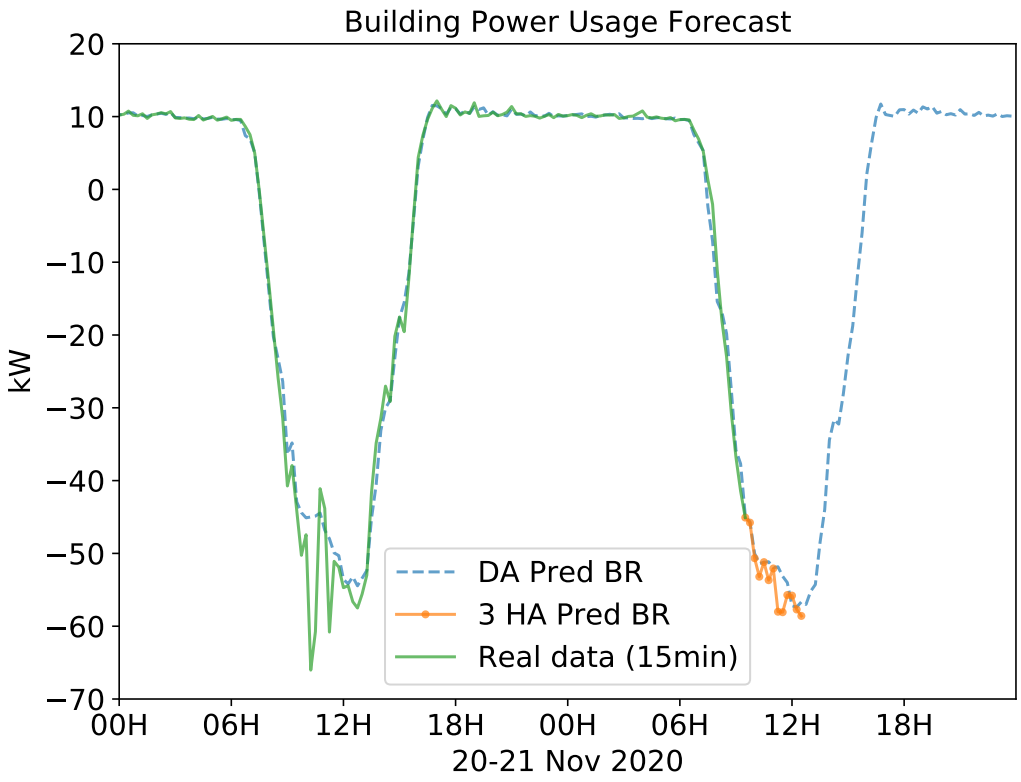

Figure 3.10: Building power usage forecast. Day-ahead (dashed blue line) and three-hour-ahead (dotted orange line) for November 21^{st} 2020. "BR" means best Random Forest model which includes the results of the cross-validation.

be capturing the underlying trend very well resulting in underfitting.

Table 3.2: Hour-ahead (HA) and day-ahead (DA) error metrics of the random forest model when predicting:

	CO_2 emissions rate ($mTCO_2/MWh$)		Solar PV Power (kW)		Building Power Usage (kW)	
	R^2	$RMSE$	R^2	$RMSE$	R^2	$RMSE$
HA	0.986	0.0084	0.969	5.9657	0.927	7.3307
DA	0.987	0.0083	0.970	5.8941	0.931	7.1568

3.4.3 Carbon-based Electric Vehicle Charging Pricing Predictions

Figure 3.11 compares the proposed carbon-based pricing, calculated and predicted, with current TOU charges. Day-ahead (DA) and three-hour-ahead (3 HA) carbon-based pricing predictions are presented for November 21st 2020, while real time calculated price is presented until 9:45am of November 21st 2020. A difference of about 0.005 $/kWh is observed overall which is defined as carbon contribution. As an example, if we assumed that an EV consumes 33 kWh to travel 100 miles [91] and the charge considering only off-peak TOU (November 21st 2020), the cost per mile is about $0.0249. However, when our carbon-based pricing is considered for the same day (excluding solar PV power), the cost per mile increases to $0.0257 during solar hours and $0.0270 for the rest of the day approximately. A larger difference in pricing is observed when we consider the solar PV power generated at CE-CERT. This is presented as our final carbon-based pricing in Figure 3.12. The carbon-based pricing incorporates local solar PV generation which is presented as a savings using a shaded area in Figure 3.12. This means that the cost per mile decreases from $0.0257 to $0 during solar hours for November 21st 2020 according to our predictions.

3.5 Chapter Conclusions

To ensure consistent pricing in EV charging, this chapter proposed a carbon-based pricing strategy and day-ahead and three-hour ahead pricing predictions. These take into account CO_2 emission rates from the grid, CAP, TOU rates, building power usage, and renewable energy generation at CE-CERT. This innovative, data-driven approach is designed

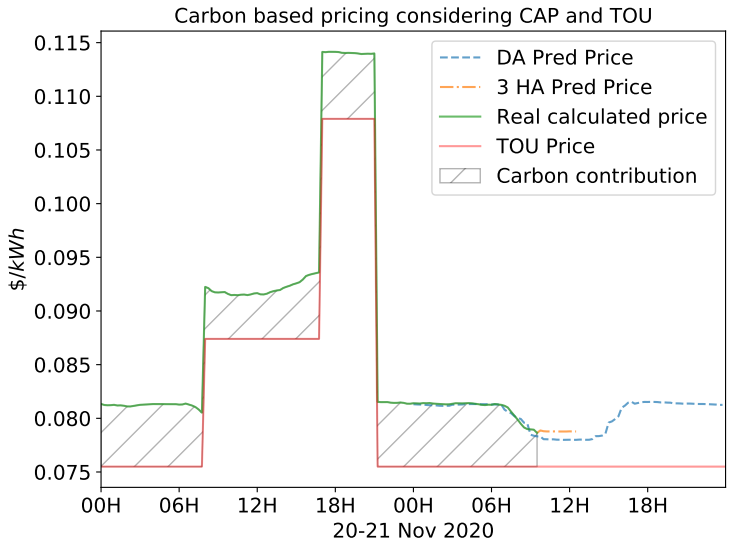

Figure 3.11: Carbon-based pricing prediction for November 21st 2020 where: "DA Pred Price" corresponds to the day-ahead predicted price in $/kWh, "3 HA Pred Price" corresponds to the three-hour-ahead predicted price in $/kWh, "Real calculated price" corresponds to the price using real time data, "TOU Price" is the TOU price, and the shaded area corresponds to the difference between TOU price and our proposed carbon-based pricing (excluding solar PV power from CE-CERT).

to shift load patterns and encourage smarter charging behavior. Demonstrating the effectiveness of controlled electric vehicle charging strategies influenced by carbon pricing, this chapter lays the groundwork for future research to further explore and refine these concepts. The model, while currently offering day-ahead and three-hour-ahead predictions, is flexible enough to be adapted for longer-term forecasts, dynamically learning from data. The three-hour-ahead forecasts are designed to adjust in real time to changes, such as weather fluctuations, ensuring adaptability. Furthermore, the model can generate weekly, monthly, and seasonal predictions, providing a comprehensive tool for managing EV charging in alignment with environmental and energy goals.

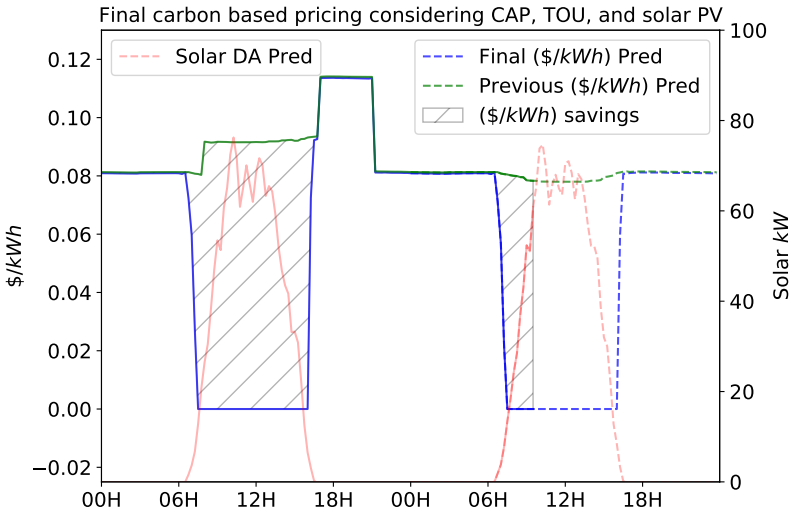

Figure 3.12: Final carbon-based pricing prediction for November 21st 2020 where: "Final ($/kWh) Pred" corresponds to the final carbon pricing considering the solar PV generation from CE-CERT, "Previous ($/kWh) Pred" is the same information presented in Figure 3.11, "Solar DA Pred" is the same information shown in Figure 3.9, and the shaded area corresponds to the difference between our carbon-based pricing with and without the solar contribution of CE-CERT.

Chapter 4

Intelligently Controlled Charging Model for BETs Considering Trip-and-Tour Patterns

Chapter 3 presented an indirect controlled electric vehicle charging strategy influenced by carbon pricing. This chapter highlights the dissertation's progression into more specific and advanced applications of controlled charging strategies, focusing on intelligent controlled charging techniques applied to BETs. Figure 4.1 summarizes the framework of this chapter.

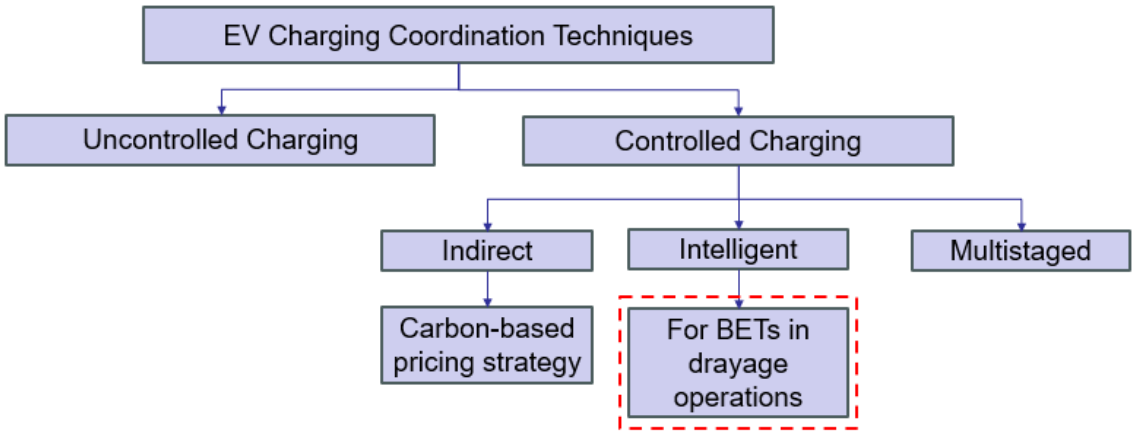

Figure 4.1: Framework of this chapter.

4.1 Introduction and Background

California has set a goal to achieve carbon neutrality by 2045, with a specific target to make all drayage trucks operating in the state be zero-emission vehicles by 2035. Achieving this target requires accurate modeling of the quantities, locations, and load profiles of chargers needed to meet statewide electrification goals. However, there are significant gaps in the current literature regarding in depth analysis of drayage truck operations, stop locations, and energy consumption. Furthermore, the development of intelligent charging models specifically for HD trucks is notably lacking.

4.2 Chapter Problem Statement

Given these gaps and existing limitations, this research:

- Proposes a data-driven methodology to identify trip-and-tour activity patterns for potential en-route opportunity charging of BETs in drayage operations at the San

Pedro Bay ports;

- Adapts BET energy efficiency in the current literature as applied to loaded and unloaded conditions; and
- Simulates charging scenarios at different locations to determine SOC with and without en-route opportunity charging for example drayage trucks based on two different charging power levels.

In addition, to efficiently project the required charging infrastructure and develop innovative solutions to meet the increasing charging demand from HD BETs, an intelligently controlled charging model was developed and evaluated using real-world activity data of drayage trucks at the Ports of Los Angeles and Long Beach. The main contributions are listed below:

- This intelligently controlled charging model is specifically designed for BETs, which takes into account TOU energy cost rates to optimize subsequent tour completion and minimize charging costs, representing a pioneering approach in BET charging.
- This model's application was demonstrated by generating home base load profiles, analyzing one year worth of real-world activity data from a fleet of 20 drayage trucks operating at the Ports of Los Angeles and Long Beach. The modeled trucks have a battery capacity of 565 kWh and are charged using a 150 kW power level.
- A sensitivity analysis was performed to compare the results of three scenarios–with 5%, 50%, and 80% reserved SOC after completing the subsequent tour.

4.3 Methodology

4.3.1 Identifying Trips and Tours using Two Stage Unsupervised ML k-Means Clustering Model

Truck activity data were analyzed for 2200 vehicles operating at the San Pedro Bay Ports terminal regions in Long Beach and Los Angeles from July 2021 to August 2022. The available data for each truck included ID (TruckId), latitude, longitude, and GPS date/time. Furthermore, data for each truck at different terminal regions were also available, including the terminal name, tract name, enter date/time to the terminal, and exit date/time from the terminal. The frequency of the activity data was not uniform as the vehicle position and GPS date/time were recorded only when the trucks moved along the road. Hence, no data were recorded if there was no movement. This fleet typically covers routes in Los Angeles, San Bernardino, and Riverside counties, as illustrated in Figure 4.2.

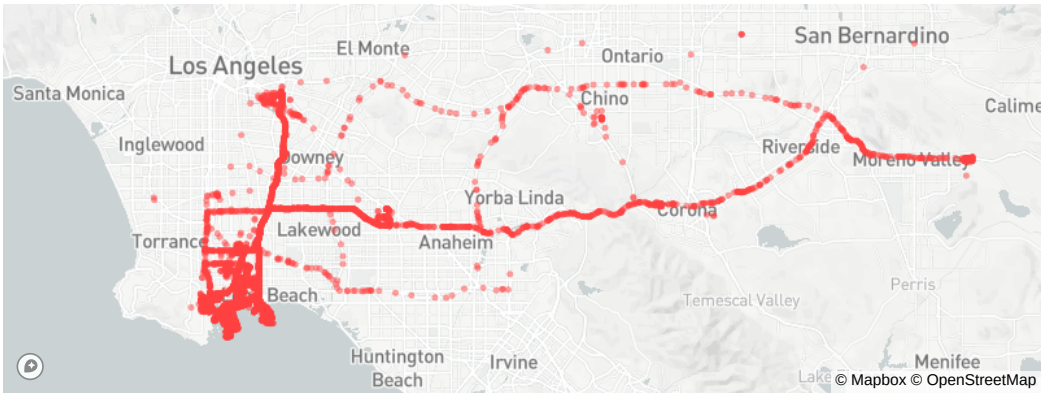

Figure 4.2: Typical routes for a fleet of 20 drayage trucks.

As shown in Figure 4.3, the data provided were pre-processed and filtered by terminal region and truckID. Additionally, the GPS date time differential was calculated to

get the time gap between each timestamp. Thus, a cluster of data points on the map with large time elapsed between timestamps would mean a potential home-base or warehouse where the truck stopped to rest or to load or unload cargo.

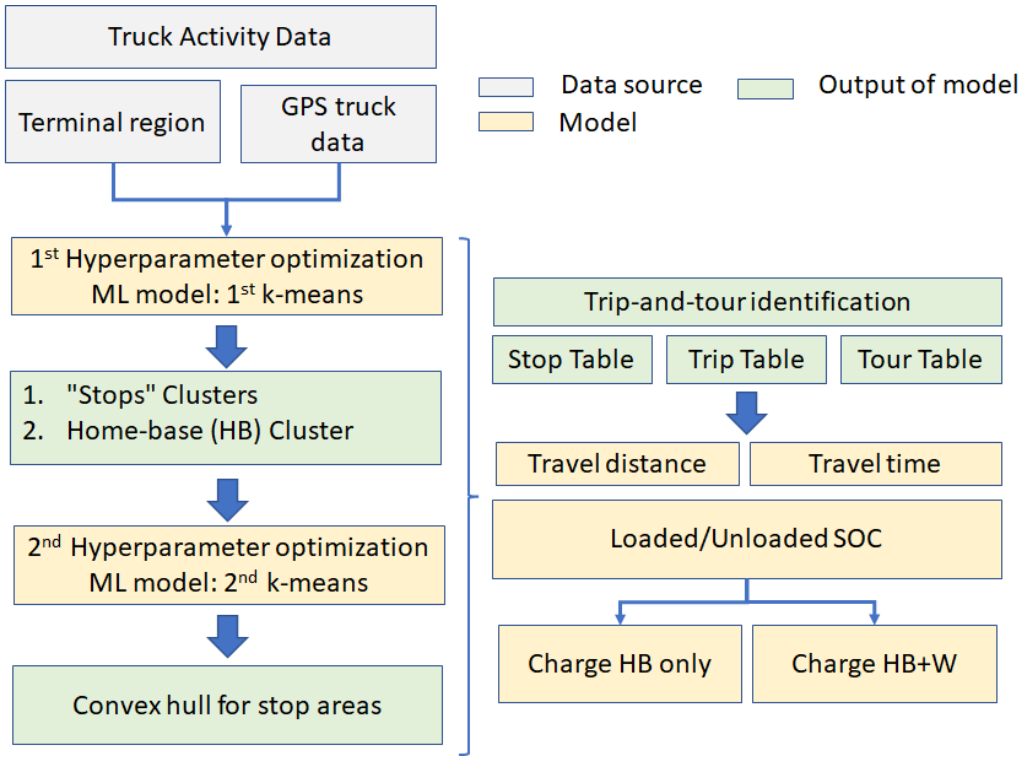

Figure 4.3: Proposed methodology. Light orange boxes correspond to models created, grey boxes correspond to data sources, and green boxes correspond to output of the models.

To isolate the stops and home-base clusters where the truck spent more time, an unsupervised k-Means ML model was implemented in Python. The k-Means algorithm clusters data by separating them in groups while minimizing the inertia [90]. This algorithm has been widely used across a range of applications mostly because its scalability, including freight GPS data analyses [92]. In addition, a hyperparameter optimization was also conducted to determine the optimal number of clusters for the initial k-Means by calculating

the average time differential and the 99th percentile in minutes for the cluster designated for removal.

After identifying potential truck stops and the home base using the first k-Means, a second k-Means model was implemented. The main aim was to obtain the convex hulls for each cluster to identify possible truck stops. Therefore, based on the original activity of the truck, every time the truck enters a convex hull and spends a significant amount of time there, the potential stop will be labeled as a significant stop. Finally, a hyperparameter optimization was also performed for the second k-Means model to determine the optimum number of clusters, maximum number of iterations of the model, and random state for result repeatability. To determine the optimal number of clusters for the second k-Means model, the Elbow method (improvement in distortion declines) was used, which involves calculating the inertia. Inertia is a measure of how well a dataset is clustered by k-Means. It is calculated by measuring the distance between each data point and its centroid, squaring this distance, and then summing these squares across one cluster. A good model is characterized by low inertia and a minimal number of clusters [93, 94].

Trips and tours were generated from the identified stops and home base. A truck trip serves a specific purpose, such as picking up a container from the port or delivering it to a warehouse. A truck tour consists of a sequence of truck trips. In this study, a truck tour is defined as starting and ending at the home base location. Tour travel distances for each truck were determined using a maps, routing, and navigation Application Programming Interface (API) in Python. It is assumed that trucks were unloaded when traveling from the home base and loaded when traveling from the ports. The loaded/unloaded status was

maintained between the end of the previous tour and the beginning of the next tour. Within a tour, the status alternates between loaded and unloaded for each trip. To calculate energy consumption, energy efficiency values from [95, 96] were utilized, with loaded and unloaded trucks consuming 3.72 kWh/mi and 1.48 kWh/mi, respectively.

4.3.2 Intelligently Controlled Charging Model

Truck activity data were analyzed for 20 vehicles belonging to the same fleet operating at the San Pedro Bay Ports terminal regions in Long Beach and Los Angeles from July 2021 to August 2022. After identifying trip-and-tour patterns, an intelligently controlled charging model for BETs that minimizes charging costs while optimizing subsequent tour completion is presented. Home base charging load profiles were generated using the proposed charging model, subject to constraints of the energy needed to complete the next subsequent tour and Time-of-Use energy cost rates. A sensitivity analysis evaluated three scenarios: a passive scenario with a 5% state-of- charge (SOC) constraint after completing the subsequent tour, an average scenario with a 50% SOC constraint, and an aggressive scenario with an 80% SOC constraint.

4.3.2.1 Objective function and Constraints

The intelligently controlled charging model optimizes charging resources such as energy cost and efficiency based on various constraints, including grid energy demand, battery capacity, network structure, and transformer efficiency, using data-driven approaches [5]. After processing trip and tour data for each truck, as well as their respective timestamps for entering and exiting the home base location, an intelligent controlled charging model

for our fleet scenario is proposed.

1. **Setup and Assumptions:** The following assumptions were made for the model:

   - Each truck has a nominal battery capacity of 565 kWh, with 80% usable capacity for SOH protection purposes [6];
   - The truck battery is 100% charged at the beginning of the first tour;
   - Charging is modeled using a 150 kW charger, and assuming a 85% charging efficiency adapted from [97];
   - When the time at the home base exceeds 24 hours, the charging session will occur during the first 24 hours;
   - The electrical load profile modeled at the home base only considers the charging of BETs.
   - The effects of temperature conditions are neglected;
   - Battery degradation and battery cell imbalance during charging are neglected;

2. **Objective Function:** Goal is to minimize the total charging cost and maximize subsequent tour completion by optimizing the charging time. Thus, for the objective function described in Equation 4.1, the charging time t in hours for each hour j and tour i is given by:

$$\text{Minimize} \sum_{i=1}^{n}\sum_{j=1}^{m} \begin{bmatrix} TOU_{ij} \\ \vdots \\ TOU_{nm} \end{bmatrix} \cdot \eta_c PL \times \begin{bmatrix} t_{ij} \\ \vdots \\ t_{nm} \end{bmatrix} \tag{4.1}$$

With: $t_{ij} \in R^n$

3. **Constraints:**

- Setting lower bounds:

$$\text{C1: } t_{ij}, \ldots, t_{nm} \geq 0 \tag{4.2}$$

- Setting upper bounds:

$$\text{C2: } [t_{ij}, \ldots, t_{nm}] \leq [K_{ij}, \ldots, K_{nm}] \tag{4.3}$$

- The total charging time should not exceed the maximum battery capacity:

$$\text{C3: } t_{ij} + \ldots + t_{nm} \leq T_i \tag{4.4}$$

- After charging, the SOC minus the energy for the next tour should meet the SOC constraint:

$$\text{C4: } \frac{(BR_i + (C3) \times \eta_c PL) - E_{i+1}}{0.8 \times BC} \geq SOC_c \tag{4.5}$$

Where:

t=charging time in hours;

i= number of the tour;

n= total number of tours;

j= hourly bin to charge at each tour;

m= total number of hours (bins) available at the home base to charge;

η_c= charging efficiency equals to 0.85;

PL= charging power level at the home base equals to 150 kW;

BC= truck battery capacity equals to 565 kWh;

K_{ij}= time remaining in hours to charge within the hourly bin (≤ 1);

T_i= time needed in tour i to have a fully charged battery in hours;

BR_i= battery remaining after tour i;

E_{i+1}= kWh needed to cover subsequent tour $(i+1)$;

SOC_c= Model constraints of 5%, 50%, and 80% represent the reserved SOC after completing the subsequent tour $(i+1)$; and

TOU_{ij}= TOU-EV-9 rate is applied for each tour i and hour j at the home base, which is located in a zipcode covered by Southern California Edison (SCE). The specific TOU rates are summarized in Table 4.1.

Table 4.1: 2019-2023 TOU-EV-9 rates SCE [8, 9]

Energy Charge	Description	$/kWh
Summer on-peak	Jun 1 - Sep 30 weekdays 4:00pm-9:00pm	0.412
Summer mid-peak	Jun 1 - Sep 30 weekends-holidays 4:00pm-9:00pm	0.218
Summer off-peak	Jun 1 - Sep 30 any other time	0.102
Winter mid-peak	Oct 1 - May 31 4:00pm-9:00pm	0.250
Winter off-peak	Oct 1 - May 31 00:00am-8:00am and 9pm-00am	0.107
Winter super-off-peak	Oct 1 - May 31 8:00am-4:00pm	0.067

4. **Optimization Technique:** The proposed algorithm shown in Algorithm 1 defines an optimization problem using the Python PuLP library [98]. PuLP is a free, open-source software written in Python. It is primarily used to describe optimization problems as mathematical models. Once defined, PuLP can call various external linear program-

ming solvers, such as CBC, GLPK, CPLEX, Gurobi, etc., to solve the model. The model uses the CBC (Coin-or branch and cut) solver. This is an open-source solver that comes bundled with PuLP. For many standard problems, particularly smaller ones, CBC is quite effective. Other solvers like Sequential Least Squares Quadratic Programming (SLSQP) and Nelder-Mead are available in the Scipy.optimize Python package [99]. These two solvers are particularly effective for non-linear optimization problems. While SLSQP is straightforward to use, Nelder-Mead does not enforce constraint handling.

The optimization problem is set up as a minimization problem with the objective function defined as the dot product of the TOU rates, power levels, and t_{ij} variables, which represent the amount of time spent charging in hourly bins. The variables are created as a dictionary using the LpVariable method, and the lowBound parameter is set to 0 to ensure non-negativity. The algorithm then sets up several constraints related to the variables, including upper bounds on the charging time and a constraint on the reserved SOC of the battery after the next subsequent tour. Finally, the optimization problem is solved using the solve method of the LpProblem class.

5. **Results:** The outcome provides the optimal charging duration for each hourly bin to construct the home-base charging load profile.

4.3.3 Home-Base Charging Load Profiles

Drayage truck activity patterns were obtained for a fleet of 45 diesel trucks operating at the ports of Los Angeles and Long Beach for a typical summer week starting on

Algorithm 1 Intelligent controlled charging algorithm

$Lp_{prob} \leftarrow p.LpProblem('Problem', p.LpMinimize)$

$t_{array} \leftarrow [\ ]$

for $i \leftarrow 1$ to n **do**

  for $j \leftarrow 1$ to m **do**

    $t[ij] \leftarrow p.LpVariable("t_{ij}", lowBound = 0)$

    $Lp_{prob} \leftarrow [TOUij] \cdot \eta_c PL \times [t_{ij}]$

    $Lp_{prob} \leftarrow tij \leq kij$

  end for

end for

return t_{array}

for $i \leftarrow 1$ to n **do**

  $Lp_{prob} \leftarrow p.lpSum(t_{array}) \leq Ti$

  $Lp_{prob} \leftarrow \frac{(BR_i + (p.lpSum(t_{array}) * \eta_c PL) - E_{i+1})}{0.8 \times BC} \geq SOC_c$

  $status \leftarrow Lp_{prob}.solve()$

end for

return t_{array}

Monday August 2nd to Sunday August 8th, 2021. After getting activity patterns for each truck and travel distances, the home-base charging load profiles for three scenarios were modeled. For the load profiles the following assumptions were made:

- Each truck was modeled using a battery capacity of 565 kWh with an 80% state-of-health protection [6];

- Charging was modeled using a 50 kW and 150 kW chargers neglecting charging losses and assuming a constant energy flow during the charging session;
- The kWh consumed during each tour were aggregated in hourly bins to get kW at 1-hour intervals;
- The last tour for each truck was removed as there was no information about the kWh that needed to be charged to cover the next subsequent tour; and
- Finally, there is no constraint related to number of chargers available. and there is no other baseloads at the home-base. Thus, the load profile modeled at the home base only considers energy charging of BETs.

4.3.3.1 Scenario 1: Baseline charging model

The home-base baseline charging scenario (Scenario 1) models the case when the trucks charge upon arrival at the home base aiming to always have a fully charged battery. This can be seen as an uncontrolled/unconstrained charging scenario. Equation 4.6 shows the energy charged at the home-base for each truck k and tour i.

$$EC_{k,i} = \begin{cases} (0.8 \times BC) - \overbrace{(BEC_{k,i-1} - ET_{k,i})}^{\text{after tour}}, \\ \qquad \Rightarrow \text{if } (CPL \times THB_{k,i}) \geq (0.8 \times BC) - (BEC_{k,i-1} - ET_{k,i}) \\ (CPL \times THB_{k,i}), \\ \qquad \Rightarrow \text{if } \underbrace{(CPL \times THB_{k,i})}_{\text{energy available}} < \underbrace{(0.8 \times BC) - (BEC_{k,i-1} - ET_{k,i})}_{\text{energy needed}} \end{cases} \tag{4.6}$$

Where:

$EC_{k,i}$ = energy charged at the home-base for each truck k and tour i;

BC = battery capacity equals to 565 kWh;

$BEC_{k,i}$ = battery energy consumption in kWh for each truck k and tour i;

$ET_{k,i}$ = energy consumed at each tour in kWh for each truck k and tour i;

CPL = charger power level of 50 kW or 150 kW;

$THB_{k,i}$ = time at the home-base in hours for each truck k and tour i.

4.3.3.2 Scenario 2: Tour completion+TOU-EV-9 rates constraints

This constrained charging scenario considers the energy needed to complete the next subsequent tour and also using TOU rates. As the home-base is located on a zipcode covered by SCE, the Summer TOU rate used corresponds to TOU-EV-9 to charge MD and HD EVs with a maximum demand higher than 500 kW, as shown in Table 4.1 [8]. As presented in Equation 4.7, this model considers subsequent tour completion and TOU-EV-9 rates. In this scenario, the truck is charged only during off-peak energy rates. In the event of not having enough energy to cover the next subsequent tour, the truck will be charged regardless of the TOU price.

Where:

$ET_{k,i+1}$ = energy to cover next tour in kWh for each truck k and tour i;

$TOU_{k,i}$ = TOU-EV-9 rate in \$/kWh for each truck k and tour i;

op = off-peak TOU-EV-9 rate in \$/kWh

$$EC_{k,i} = \begin{cases} 0, & \text{if } \overbrace{(BEC_{k,i-1} - ET_{k,i})}^{\text{after tour}} \geq ET_{k,i+1} \text{ and } (TOU_{k,i} \neq op) \\ ET_{k,i+1}, & \text{if } (BEC_{k,i-1} - ET_{k,i}) \geq ET_{k,i+1} \text{ and } (TOU_{k,i} = op) \\ & \text{and } (CPL \times THB_{k,i} ET_{k,i+1}) \\ ET_{k,i+1} - (BEC_{k,i-1} - ET_{k,i}), & \text{if } (CPL \times THB_{k,i} \geq ET_{k,i+1} - (BEC_{k,i-1} - ET_{k,i}) \\ (CPL \times THB_{k,i}), & \text{if } \underbrace{(CPL \times THB_{k,i})}_{\text{energy available}} < \underbrace{ET_{k,i+1} - (BEC_{k,i-1} - ET_{k,i})}_{\text{energy needed}} \end{cases} \tag{4.7}$$

4.3.3.3 Scenario 3: Tour completion constraint

Similarly, for the Scenario 3, we only consider subsequent tour completion, as presented in Equation 4.8. This means, that if the truck has enough battery to cover the next subsequent tour, there is no charging. In case of insufficient energy to cover the next subsequent tour, the truck will be charged based on the energy available.

$$EC_{k,i} = \begin{cases} 0, & \text{if } \overbrace{(BEC_{k,i-1} - ET_{k,i})}^{\text{after tour}} \geq ET_{k,i+1} \\ ET_{k,i+1} - (BEC_{k,i-1} - ET_{k,i}), & \text{if } (CPL \times THB_{k,i} \geq ET_{k,i+1} - (BEC_{k,i-1} - ET_{k,i}) \\ (CPL \times THB_{k,i}), & \text{if } \underbrace{(CPL \times THB_{k,i})}_{\text{energy available}} < \underbrace{ET_{k,i+1} - (BEC_{k,i-1} - ET_{k,i})}_{\text{energy needed}} \end{cases} \tag{4.8}$$

After getting the energy charged at the home-base for each scenario and truck

and tour combination (i, k), energy was distributed into one-hour intervals to create the aggregated charging load profile and multiplied by the corresponding TOU-EV-9 rate to get the energy cost, percentage of tours completed, and number of chargers needed.

4.3.4 En-Route Opportunity Charging

Activity data at the terminal regions of the ports of Long Beach and Los Angeles over 2 days (August 2-3, 2021) were analyzed for two selected trucks (Truck A and Truck B) as an initial step to assess the necessity of providing en-route opportunity charging. To calculate the SOC of the trucks, the following assumptions were made:

1. Energy performance efficiency for drayage trucks was adapted from [96]. It was assumed a 60% local and 40% freeway operation, resulting in 3.72 kWh/mi for loaded and 1.48 kWh/mi for unloaded trucks;

2. Trucks are unloaded when coming from the home-base and loaded when coming from the port. The other statuses were manually assigned;

3. Battery capacity was adapted from [6] with a usable battery capacity of 300 kWh assuming a 80% battery SOH protection;

4. 100% SOC at the beginning of the first trip; and

5. A 50 kW and 150 kW charger were used, neglecting charging losses.

Finally, two different scenarios were considered: potential en-route opportunity charging at the home-base only, and potential en-route opportunity charging at the home-base and warehouse stops.

4.4 Results and Discussion

4.4.1 Identifying Trips and Tours using Two Stage Unsupervised Machine Learning k-Means Clustering Model

4.4.1.1 k-Means Hyperparameter Optimization

The results of the sensitivity analysis for determining the optimal number of clusters are shown in Figure 4.4. For the initial k-Means, the optimal number of clusters was determined by calculating both the average time and the 99th percentile in minutes for cluster 0 situated at the bottom (as seen in Figure 4.4 middle). This cluster represents the truck constantly moving and does not indicate potential stops for the truck. This cluster was subsequently excluded from the analysis. Therefore, with 13 modeled clusters, the cluster designated for removal has a mean of 0.7 minutes, and 99% of the points stopped for 2.3 minutes or fewer (Figure 4.4 left). Increasing the total number of clusters to 14 causes 99% of the points in the cluster designated for removal to stop for 0.9 minutes or less, a duration considerably shorter than the 3-minute threshold found in the literature [71, 70]. The result of the Elbow method to determine the optimal number of clusters for the second k-Means model is shown in Figure 4.4-right.

Convex hulls computed as a results of the second k-means performed using only GPS latitude and longitude are presented in Figure 4.5.

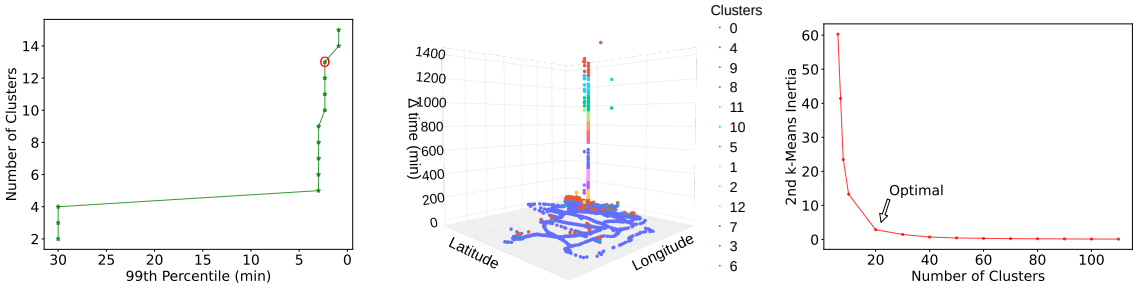

Figure 4.4: Results of the first k-Means hyperparameter optimization (left), the time differential plot (middle), and the second k-Means hyperparameter optimization (right) for a fleet of 20 trucks using data from July 2021 to August 2022. The optimal numbers of clusters for the first and second k-Means models were 13 and 20, respectively.

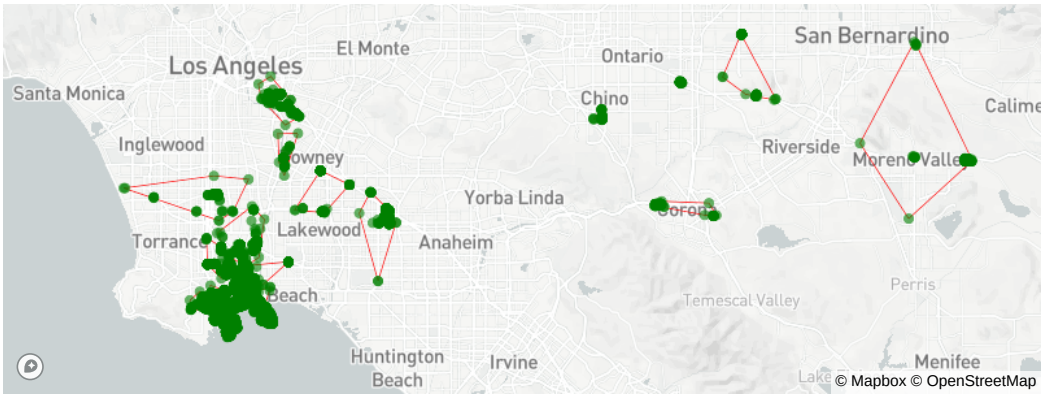

Figure 4.5: Results of applying the second k-Means model to a fleet of 20 trucks using data from July 2021 to August 2022. The 20 resulting clusters are represented by green dots and enclosed in red convex hulls. Additionally, a manual convex hull was assigned to the data to indicate the home base.

4.4.2 Intelligently Controlled Charging Model

4.4.2.1 Trip-and-Tour Identification

After obtaining the convex hulls for the stops of both trucks, trip-and-tour identification was conducted. Figure 4.6 presents a comparison of the locations visited by Trucks 0 to 19 from July 2021 to August 2022, emphasizing the variability in travel patterns across the fleet. Some trucks, such as Truck 1, display more active travel patterns, while others,

like Truck 13, show notably less activity. Moreover, it's evident that certain trucks make more intermediate stops between the home base (red dots) and the port (blue dots). This variability is further highlighted in Table 4.2, which lists the number of trips and tours per truck over one year.

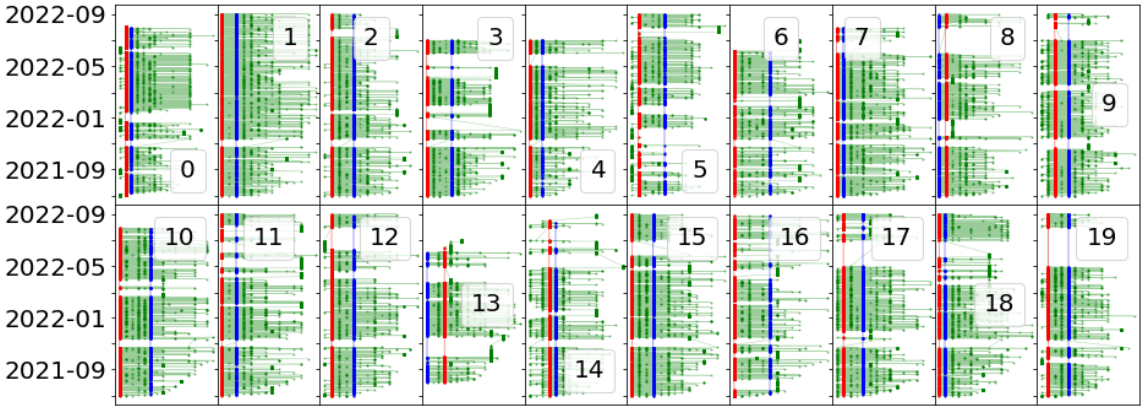

Figure 4.6: Locations visited by Trucks 0 to 19 between July 2021 and August 2022. The red dots represent a stop at the home base, while the blue dots represent a stop at the port.

Figure 4.7 displays the tour travel distance and cumulative distributions for a fleet of 20 trucks operating at the San Pedro Bay ports from July 2021 to August 2022. It is worth noting that all tours in the fleet have a travel distance less than the 275-mile range for a truck with a 565 kWh battery capacity [6]. Achieving a 275-mile range would require an assumed energy efficiency of 2 kWh per mile, but it is important to consider that drayage trucks consume varying amounts of kWh per mile depending on factors such as cargo load and road type (freeway or local) [95, 96]. Additionally, drayage trucks may not be able to begin each tour with a 100% SOC due to the limited time available for charging between consecutive tours, which underscores the need for an intelligently controlled charging model

Table 4.2: Number of tours and trips per truck for a fleet of 20 trucks using data from July 2021 to August 2022

TruckId	# of Tours	# of trip
0	369	1273
1	411	1449
2	395	1281
3	316	1148
4	308	991
5	245	816
6	224	756
7	395	1395
8	299	970
9	418	1441
10	389	1333
11	309	1043
12	309	1009
13	204	793
14	335	1072
15	389	1469
16	237	754
17	357	1356
18	303	1121
19	336	1192

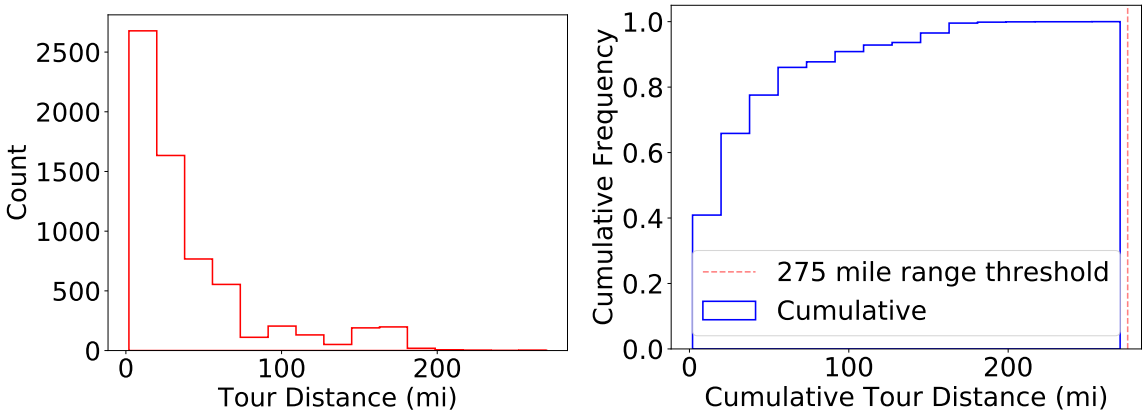

Figure 4.7: Tour distance distribution (left) and normalized cumulative tour distance (right) for a fleet of 20 trucks operating at the San Pedro Bay ports between July 2021 and August 2022. The figure also includes a threshold of 275 miles, as it has been suggested in [6] that this is the expected range for a 565 kWh battery electric truck.

4.4.2.2 Tour Completion Analysis

One of the primary constraints in the intelligently controlled charging model is the completion of subsequent tours. Table 4.2 summarizes the percentage of tours completed under the three SOC constrained scenarios.

Table 4.3: Total number of tours completed per constrained scenarios.

SOC Constraint	**N° Tours Optimal Sol.**	**N° Tours Infeasible Sol.**	**% Tours Completed**
5%	3563	153	95.9%
50%	3020	696	81.3%
80%	1806	1910	51.4%

It becomes evident that as the remaining SOC constraint becomes more aggressive, the percentage of completed tours decreases. This is due to the model lacking optimal solutions. The table also indicates the number of tours with optimal and infeasible solutions. As shown in Figure 4.8, for a truck that spends 3 hours at the home-base, each axis (t_1, t_2, t_3) represents the hourly bin to be optimized. A tour with an infeasible solution indicates that the available charging time does not satisfy the constraints in Equation 4.1, preventing the model from completing the next tour, as highlighted by the red dot being outside the cube. Consequently, a scenario with 5% reserved SOC after completing the subsequent tour will result in 96% of tours being completed across the entire fleet. Results from Tanvir et al. [67] indicate that BETs might complete up to 85% of the tours when opportunity charged at the home base between consecutive tours. In light of this, our intelligently controlled charging model suggests a potential to increase the tour completion rate to as much as 96%. Furthermore, when juxtaposing the results with the normalized cumulative tour distance

for this fleet (Figure 4.7), it implies that all tours should be completed. However, there remain about 153 tours (4%) that will not be completed in one year.

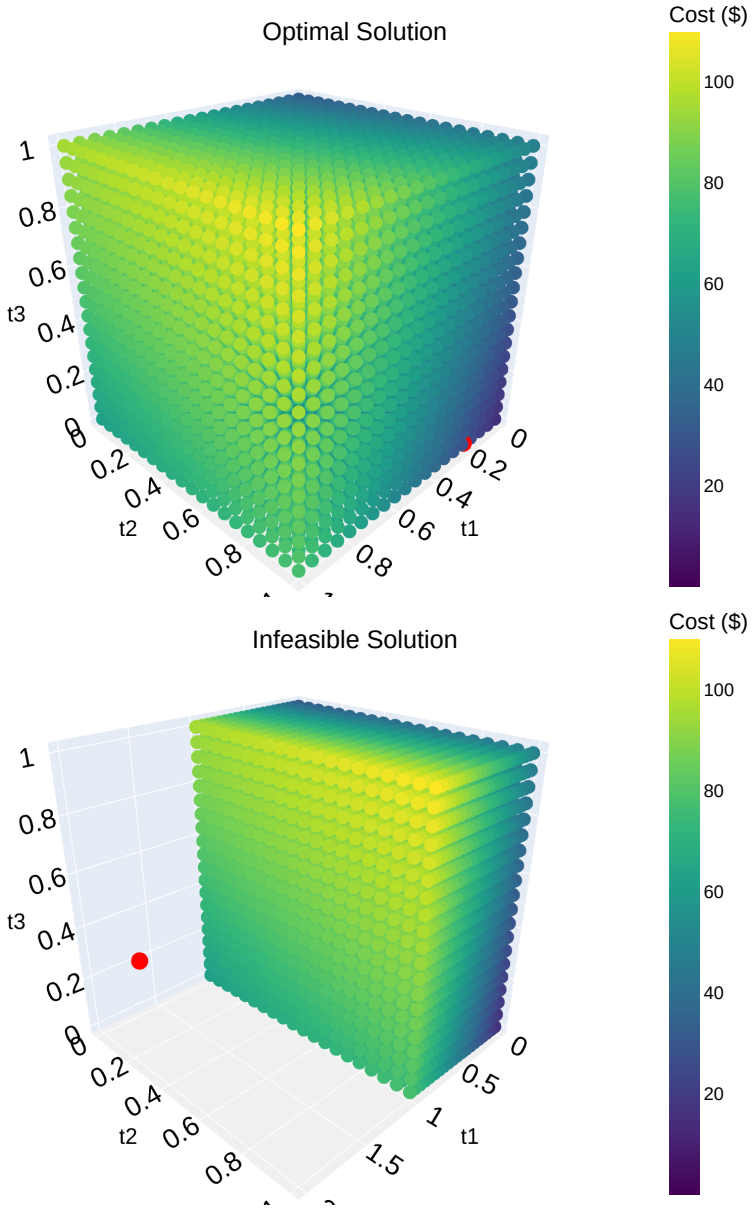

Figure 4.8: Optimal (top) vs. Infeasible (bottom) solutions from the optimization model for a truck that spends 3 hours at the home-base. Each axis (t_1,t_2,t_3) represents the hourly bin that needs to be optimized. Colormap represents the charging cost in $. Red dot represents the solution given by the optimization model.

The percentage of tours completed by each truck under the three modeled scenarios is presented in Figure 4.9. It is evident that certain trucks completed more tours than others. For example, while TruckId 11 and 12 both embarked on the same number of tours (as detailed in Table 4.2), they differed in the number of trips made, with 1043 and 1009 trips, respectively. This variation in trips leads to a distinct energy consumption pattern, influenced by the route taken by the truck and whether it is carrying cargo or not.

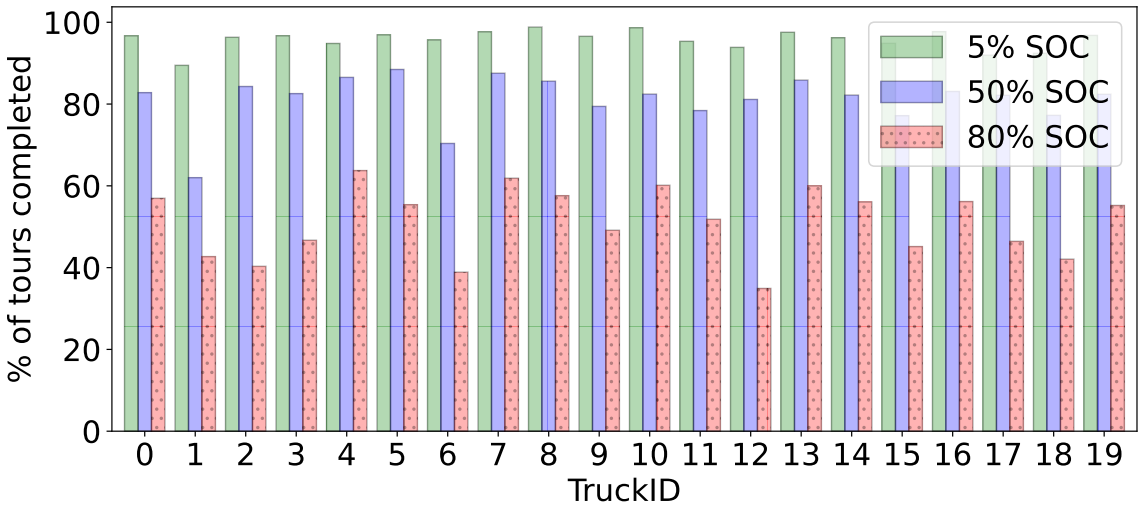

Figure 4.9: Percentage of tours completed per truck under the three modeled scenarios for a fleet of 20 trucks operating at the San Pedro Bay ports between July 2021 and August 2022.

4.4.2.3 Home-Base Load Analysis

Figure 4.10 displays the hourly home base load profile in kW generated by the intelligent controlled charging model under the three remaining SOC constraints. This zoomed-out figure highlights the 5% SOC constraint.

The daily aggregated load profile per month in kW, under the three different

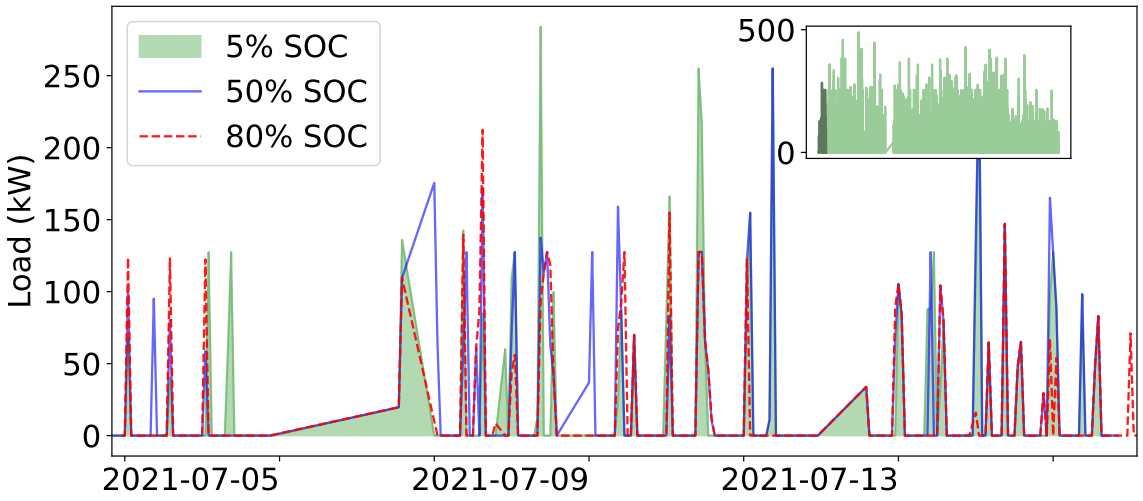

Figure 4.10: Hourly home base load profile in kW generated for the month of July 2021 for a fleet of 20 trucks using the intelligent controlled charging model with three SOC constraints. The zoom-out figure presents the hourly profile from July 2021 to August 2022 for the 5% SOC constrained scenario.

scenarios considered, is presented in Figure 4.11. A seasonality pattern within each month is evident. Patterns corresponding to weekdays are noticeable every approximately five days, representing truck charging during the weekdays and minimal charging over the weekends. Furthermore, a load seasonality in the energy charged can be observed during the Summer months of July and August 2021. This seasonality might also be linked to the type of product the drayage truck transports and its import patterns to the country during specific months of the year. Comparing the three constrained SOC scenarios, the variability introduced by the available charging time at the home base, and subsequently, the number of feasible solutions is evident. This variability is highlighted by the vertical gap in kW between the 5%, 50%, and 80% cases.

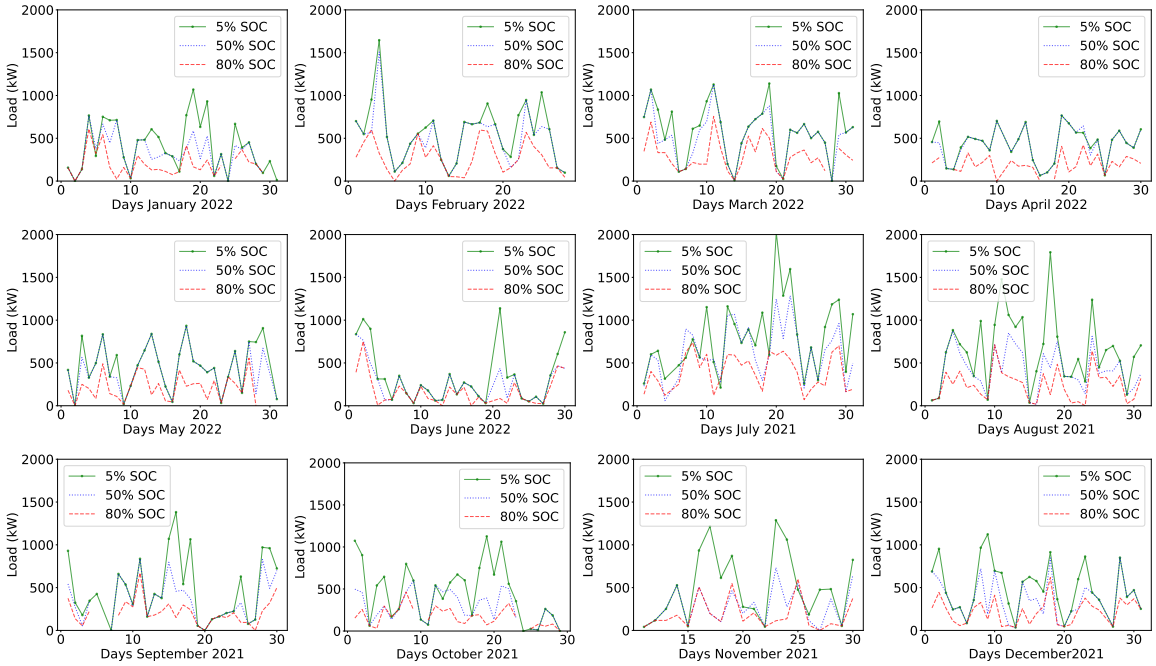

Figure 4.11: Aggregated daily load profile per month at the home base in kW for a fleet of 20 trucks using data from July 1, 2021 to June 30, 2022, showing a one-year seasonality.

4.4.2.4 Cost Analysis

Figure 4.12 presents a comparison of the cumulative charging costs from July 2021 to August 2022 for the three SOC constrained scenarios using the TOU-EV-9 rates detailed in Table 4.1. The total cumulative charging cost for one year under the 5% SOC constraint amounts to approximately $33,000, as outlined in Table 4.4. However, when contrasted with the 80% SOC scenario, a decrease of 34% in charging cost (from $33,174 to $11,341) is observed. Yet, this decrease does not correspond to an equivalent 44% reduction in the number of tours completed. This discrepancy arises from the optimal solutions at each tour, with the number of infeasible solutions not factored into the charging cost.

For the infeasible solutions, a delay cost of $26.7 per hour from [100] was used to

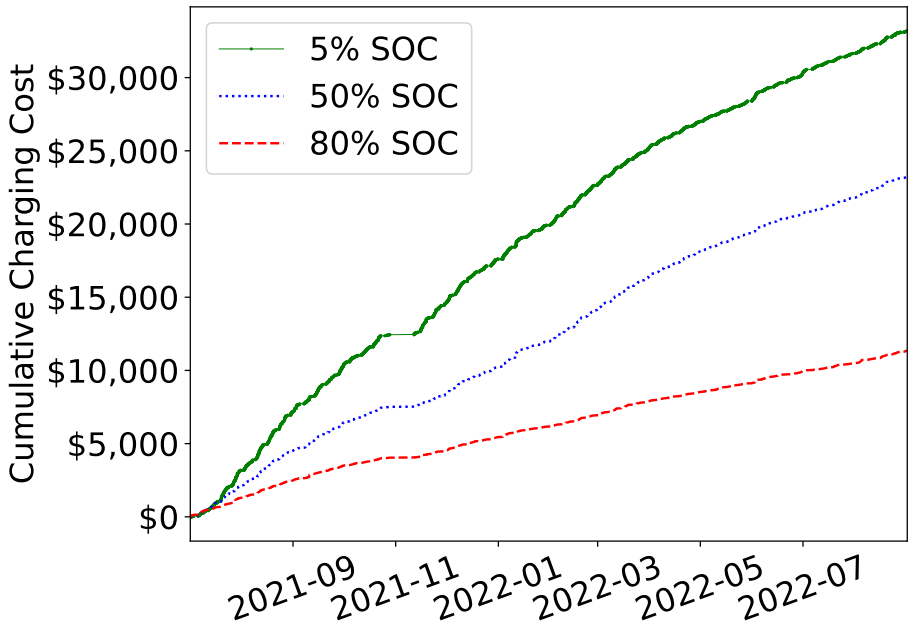

Figure 4.12: Cumulative energy charging cost using the TOU-EV-9 rates for the three SOC constrained scenarios from July 2021 to August 2022

compare optimal vs. infeasible tour solutions, with each tour being analyzed independently. Total charging vs. delay costs are presented in Figure 4.13. This clearly indicates that the scenario with 80% SOC has a significant total cost when delay is considered. Finally, the 5% SOC constraint resulted in a total charging and delay cost of about $40,000 per year, whereas the 80% SOC led to almost double that amount.

The total cost per truckId is presented in Figure 4.14. Among them, TruckId 11 stands out with notably more variability than the others. This graph serves as a valuable tool for pinpointing the trucks and routes that might benefit from earlier re-routing to diminish delay costs.

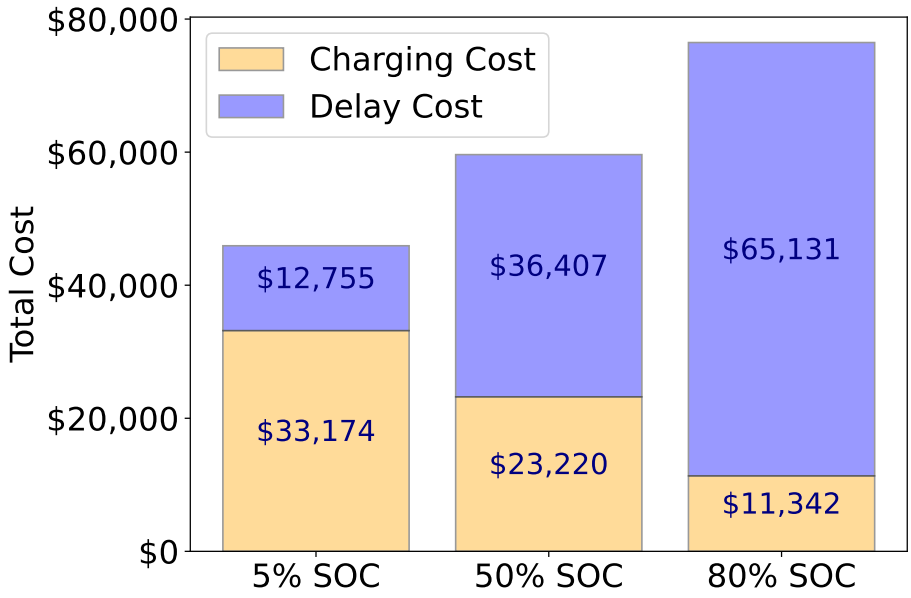

Figure 4.13: Charging vs. Delay costs for the three SOC constrained scenarios from July 2021 to August 2022.

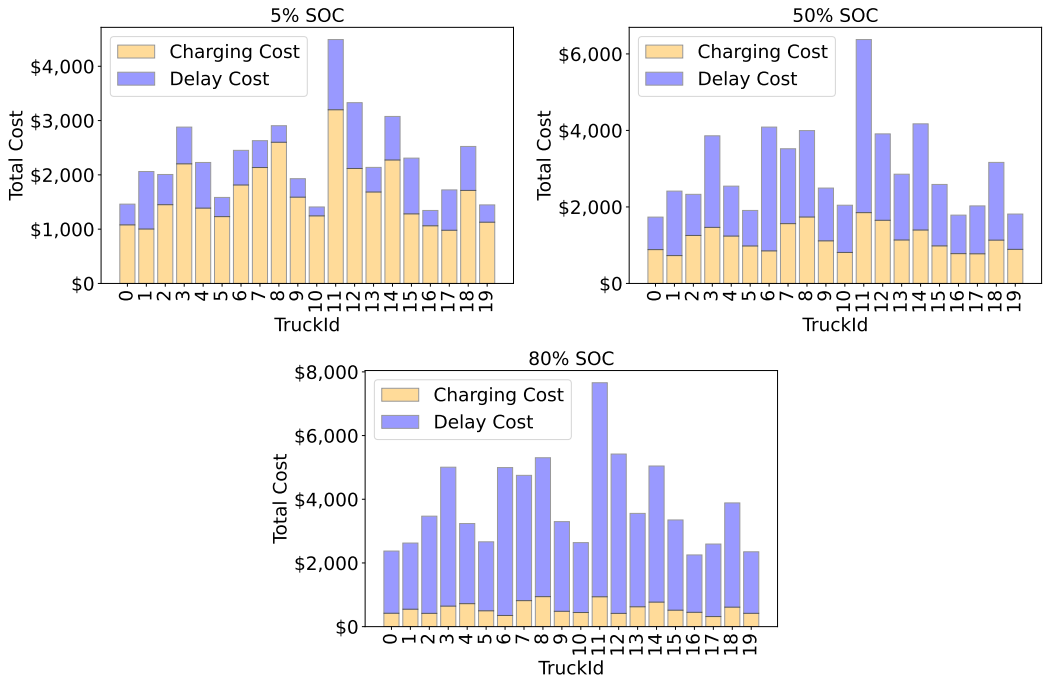

Figure 4.14: Charging vs. Delay costs for the three SOC constrained scenarios from July 2021 to August 2022 per TruckId.

Table 4.4: Monthly energy charging cost from July 2021 to August 2022 considering the three SOC constrained scenarios.

Year-Month	5% SOC	50% SOC	80% SOC
2021-07	$3,169.2	$2,137.9	$1,294.8
2021-08	$4,018.3	$2,376.9	$1,187.5
2021-09	$3,087.8	$1,896.5	$1,016.8
2021-10	$2,164.1	$1,099.1	$540.7
2021-11	$2,158.7	$868.6	$490.1
2021-12	$3,001.9	$1,870.4	$919.2
2022-01	$2,350.1	$1,757.1	$703.5
2022-02	$2,728.1	$2,143.5	$778.6
2022-03	$2,569.1	$2,326.9	$978.1
2022-04	$1,760.7	$1,659.7	$621.1
2022-05	$1,432.9	$1,270.5	$607.0
2022-06	$1,875.9	$1,336.5	$815.2
2022-07	$1,333.0	$1,056.5	$537.4
2022-08	$1,524.5	$1,419.5	$851.9
TOTAL	**$33,174.3**	**$23,219.7**	**$11,341.9**

4.4.3 Home-Base Charging Load Profiles

4.4.3.1 Home-Base Load Profile Using a 50 kW Power Level

The aggregated home-base charging load is presented in Fig. 4.15 considering a charging power level of 50 kW for the entire fleet. For this week, most of the charging occurs during off-peak TOU-EV-9 and the charging load decreased significantly over the weekend for all the modeled cases as there were no tours on Sunday August 8^{th}.

4.4.3.2 Home-Base Load Profile Using a 150 kW Power Level

Similarly, an aggregated home-base charging load is presented in Fig. 4.16 considering a charging power level of 150 kW for the entire fleet. When comparing Fig. 4.15 and Fig. 4.16, it is clearly seen the difference on the home-base load when using a higher power

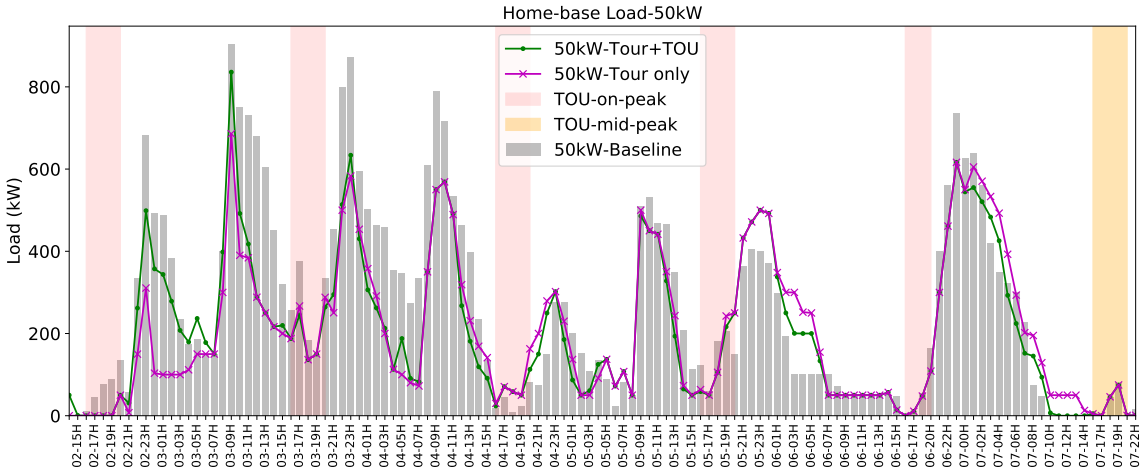

Figure 4.15: Load at the home-base from August 2nd to August 8th, 2021, using a power level of 50 kW with a battery capacity of 565 kWh. Baseline charging load scenario is shown as grey bars. Scenario 2 is showed using green line, and Scenario 3 is showed using purple line. Shaded area in red represents Summer on-peak weekday TOU-EV-9 rate, and shaded area in orange represents Summer mid-peak weekend TOU-EV-9 rate.

level, as the curves are less spread as more energy is charged per hour using a higher power level.

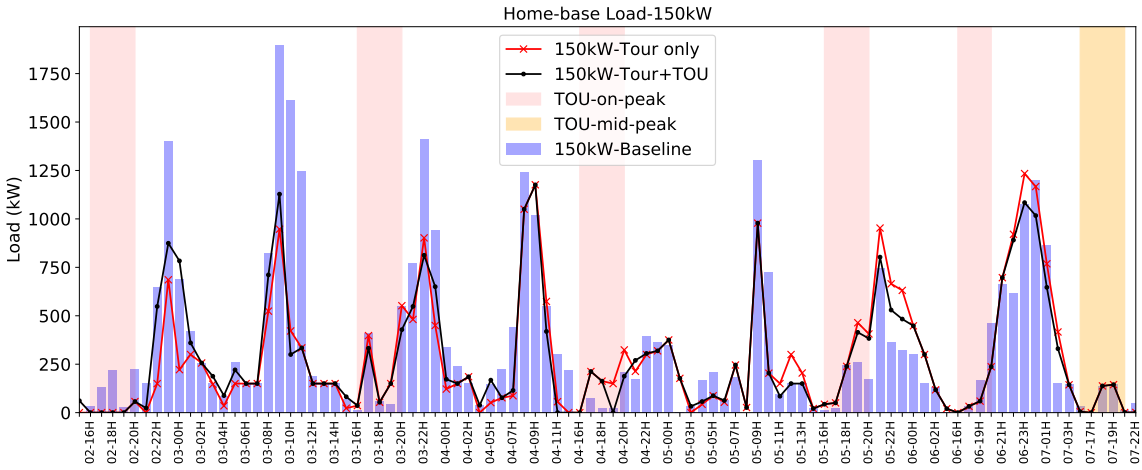

Figure 4.16: Load at the home-base from August 2nd to August 8th, 2021, using a power level of 150 kW with a battery capacity of 565 kWh. Scenario 1 is shown as blue bars. Scenario 2 is showed using black line. Scenario 3 is showed using red line. Shaded area in red represents Summer on-peak weekday TOU-EV-9 rate, and shaded area in orange represents Summer mid-peak weekend TOU-EV-9 rate.

Based on the aggregated home-base charging profile for the fleet shown in Fig. 4.15 and Fig. 4.16, it is observed that higher charging energy peaks occur in the baseline charging case (Scenario 1) with a power level of 150 kW. This is because the baseline strategy aims to always charge the battery fully with the energy available. Thus, with a higher power level, there is more energy (kWh) available per hour than using a lower power level. The home-base peak charging loads decrease in most of the days for Scenario 2 and 3 at both power levels as the trucks are not charged if they have enough energy to cover the next subsequent tour and when the energy is expensive. From the figures, it can also be concluded that the home-base energy loads of Scenario 2 (tour completion and TOU-EV-9 constraints) and Scenario 3 (only tour completion constraint) are similar. This is expected, as our model (as shown in Equation 4.7 and Equation 4.8) charges the battery enough to complete the next subsequent tour regardless of the TOU-EV-9 rate in the cases where there is not enough energy in the battery to complete the next tour. The TOU-EV-9 rate only plays a role when there is sufficient energy to complete the next tour, as we charge only when there is an off-peak TOU-EV-9 rate.

4.4.3.3 Energy Charging Cost at Different Scenarios and Power Levels

A comparison between cumulative energy charging cost using the TOU-EV-9 rate at different power levels and for the three scenarios modeled is presented in Fig. 4.17. The most expensive case corresponds to the baseline case (Scenario 1) and using a 150 kW power level charger, followed by a 50 kW power level charger. This is followed by the 150 kW Scenario 3, then the 150 kW Scenario 2. The least expensive cases uses a power level of 50

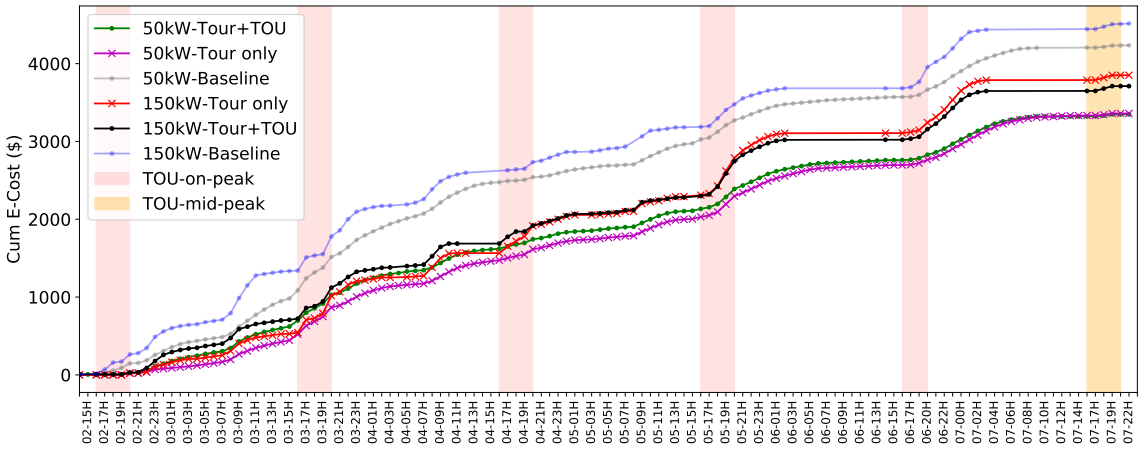

Figure 4.17: Cumulative energy charging cost when comparing 50 kW and 150 kW power levels for Scenario 1-3 for the fleet during August 2nd to August 8th, 2021.

kW in Scenarios 2 and 3. Table 4.5 summarizes the results for each modeled scenario.

Table 4.5: Summary of Results

Configuration	**% Tours Completed**	**Energy Charging Cost ($)**	**No. Chargers Needed**
50kW-baseline	0.906	4235.8	20
150kW-baseline	0.951	4515.5	16
50kW-Tour+TOU	0.768	3349.0	18
150kW-Tour+TOU	0.866	3711.1	13
50kW-Tour only	0.715	3359.9	17
150kW-Tour only	0.835	3851.0	13

In terms of energy cost, there is a decrease in the energy charging cost when comparing the baseline charging case with the other cases. In the case of 50 kW charging power, there is a 20.9% and 20.6% decrease in the energy charging cost when comparing the baseline case with Scenario 2 and Scenario 3, respectively (shown in Table 4.5). This can be clearly seen in Fig. 4.17, where these two models (green line represents Scenario 2 and purple line represents Scenario 3) present a similar cumulative energy cost over the study

period. This can be explained by the models charging the energy available rather than the energy required to complete the next subsequent tour, as when using a lower power level, there is less power available per hour to supply the energy required. Higher energy charging costs are observed when increasing the power level from 50 kW to 150 kW for both Scenario 2 and Scenario 3. A decrease in the energy charging costs of 18% and 15% are observed when comparing the baseline case with Scenario 2 and Scenario 3 respectively, using a power level of 150 kW. The decrease in energy costs is not as significant as the case when using a 50 kW power level. However, the percentage of tours completed increases by 10% in the Scenario 2 and by 12% in the Scenario 3 just by using a higher power level. Overall, the percentage of tours completed drops when compared to the baseline scenario. The baseline case always tries to fully charge the battery of the trucks, whereas Scenario 2 and 3 are highly impacted by only supplying the battery enough energy to complete the next subsequent tour. This highlights the importance of feeding the model with more look-ahead tour information, as considering only the energy to complete the next subsequent tour does not seem to be sufficient to increase the number of tours completed.

Finally, the number of chargers needed over the study period was obtained by analyzing the aggregated load profile and the number of unique trucks per hour during charging. The proposed models decrease the number of chargers needed by 2.5 and 3 on average when using a power level of 50 kW and 150 kW, respectively, when compared to their baseline cases. This metric was considered because a one-to-one charger-to-truck ratio is often suggested as a straightforward strategy for electric truck adoption [79]. Our results suggest that 13 chargers are needed when implementing the models using a power level of

150kW, which is only about one-third of the 38 chargers that would have been potentially needed if following the basic one-to-one charger-to-truck ratio strategy. Moreover, as prices for a level 2 DC charger with a power level between 50 kW-150kW can range between $50,000-$100,000 [101], strategies to reduce the number of chargers required and their cost need to be explored and included in energy cost analyses.

4.4.4 En-Route Opportunity Charging

4.4.4.1 Trip-and-Tour Identification

Figure 4.18 compares the locations that Truck A and B visited during August 2-3, 2021. It is observed that Truck A visited the port, four stops, and also the home-base for a longer period of time. On the contrary, Truck B visited the port, three stops, and its stops at the home-base were shorter.

The trip-table for Truck B from August 2-3, 2021 is presented in Table 4.6. This truck had 11 trips, represented by each row in the table, and 3 tours (from home-base to home-base) over a two day period. Cumulative travel distance was 216 miles and cumulative travel time was 5.2 hours for Truck B. On the other hand, cumulative travel distance was 118 miles and cumulative travel time was 3.6 hours for Truck A.

4.4.4.2 SOC Charging Scenarios

Figure 4.19 shows different modeled SOC scenarios for Trucks A and B. It is observed that Truck A is able to complete all the trips without requiring en-route opportunity charging (Figure 4.19-a). However, Truck B shows a different case. When modeling

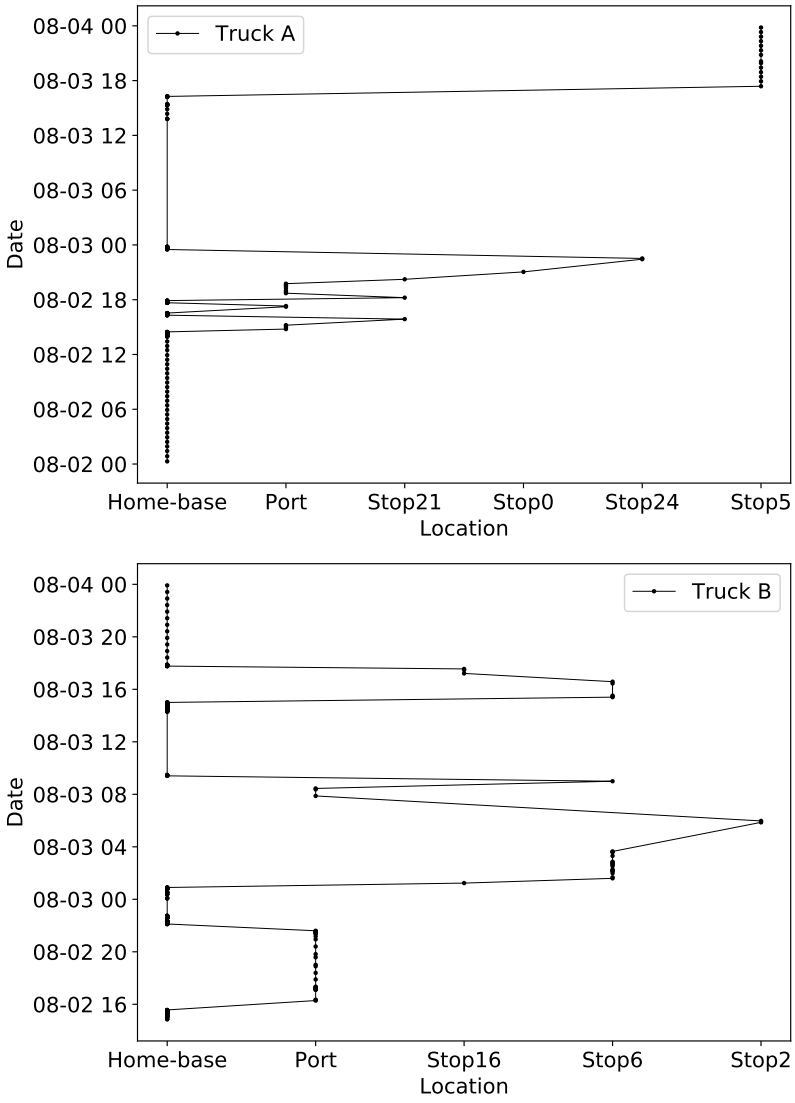

Figure 4.18: Locations visited by Trucks A (top) and B (bottom) from August 2-3 2021.

the scenario of home-base only en-route opportunity charging with a 50 kW power level (Figure 4.19-b), an improvement in the SOC is observed when compared to the no charging scenario. However, its battery will be discharged before completing the fifth trip from Stop6 to Stop2. When modifying the en-route charging scenario at home-base+Stop6, about 100 kWh were added to the battery SOC as the truck spent about 2 hours in this stop (Stop6).

Table 4.6: Trip-table for Truck B from August 2-3 2021.

Trip-Table: Truck B			
Start Location	***End Location***	***Travel distance (mi)***	***Travel time (min)***
Home-base	Port	6.854	13.403
Port	Home-base	6.830	13.238
Home-base	Stop16	4.572	8.535
Stop16	Stop6	5.441	12.032
Stop6	Stop2	82.318	97.838
Stop2	Port	76.494	102.145
Port	Stop6	8.232	18.312
Stop6	Home-base	6.946	13.747
Home-base	Stop6	8.577	14.527
Stop6	Stop16	5.507	11.697
Stop16	Home-base	4.212	7.908

Thus, the truck would be able to complete the fifth trip (Stop6 to Stop2) ending with a -2% SOC by using its reserved battery capacity, but its battery will be discharged before completing the next trip from Stop2 to the Port. Moreover, the truck did not spend enough time at Stop2, so even if some en-route opportunity charging is added at this stop (home-base+Stop6+Stop2 scenario), there is no significant improvement in SOC when using a 50 kW charger unless the truck spends more time at this stop.

Similarly, SOC scenarios were modeled for Truck B using en-route opportunity charging at a higher power level of 150 kW. For the case of charging at the home-base only (Figure 4.19-c), there is no significant difference in the SOC when using a power level of 50 or 150 kW because the truck spent enough time there to be able to fully recharge its battery. Moreover, there is no significant improvement when increasing the power level at Stop 6 from 50 to 150 kW. The truck did not consume a notable amount of energy from previous trips and it is almost fully charged before starting the fifth trip. So the truck ends

with a -2% SOC after the Stop6 to Stop2 trip, regardless of the power level that we have in Stop6 because of the travel distance of the trip. In addition, a small SOC improvement is observed when modeling the en-route opportunity charging scenario using a power level of 150 kW at Stop2. Finally, as shown in Figure 4.19 (d), Truck B will be able to complete all of its trips by using a 150 kW power level at Stop2 and by extending its stay at Stop2 from 0.11 to 1.07 hours recharging 161 kWh to its battery.

4.5 Chapter Conclusions

This chapter addressed significant gaps in the literature regarding in depth analysis of drayage truck operations and intelligent charging models. A novel methodology utilizing ML techniques to identify the activity patterns of drayage trucks has been introduced, paving the way for smarter logistics and operational efficiency. Moreover, this chapter presented an intelligently controlled charging model for BETs that aims to minimize charging costs while optimizing the completion of subsequent tours. The results are promising, indicating that maintaining a 5% SOC buffer after completing the next tour ensures 96% of tours are completed across the fleet. While the research presented here is contextualized by work at the ports of Los Angeles and Long Beach, the methodologies and models are designed with adaptability in mind, allowing for application to other ports such as Houston, Savannah, New York, etc., thereby offering a versatile solution to a global challenge in port operations and electric truck management.

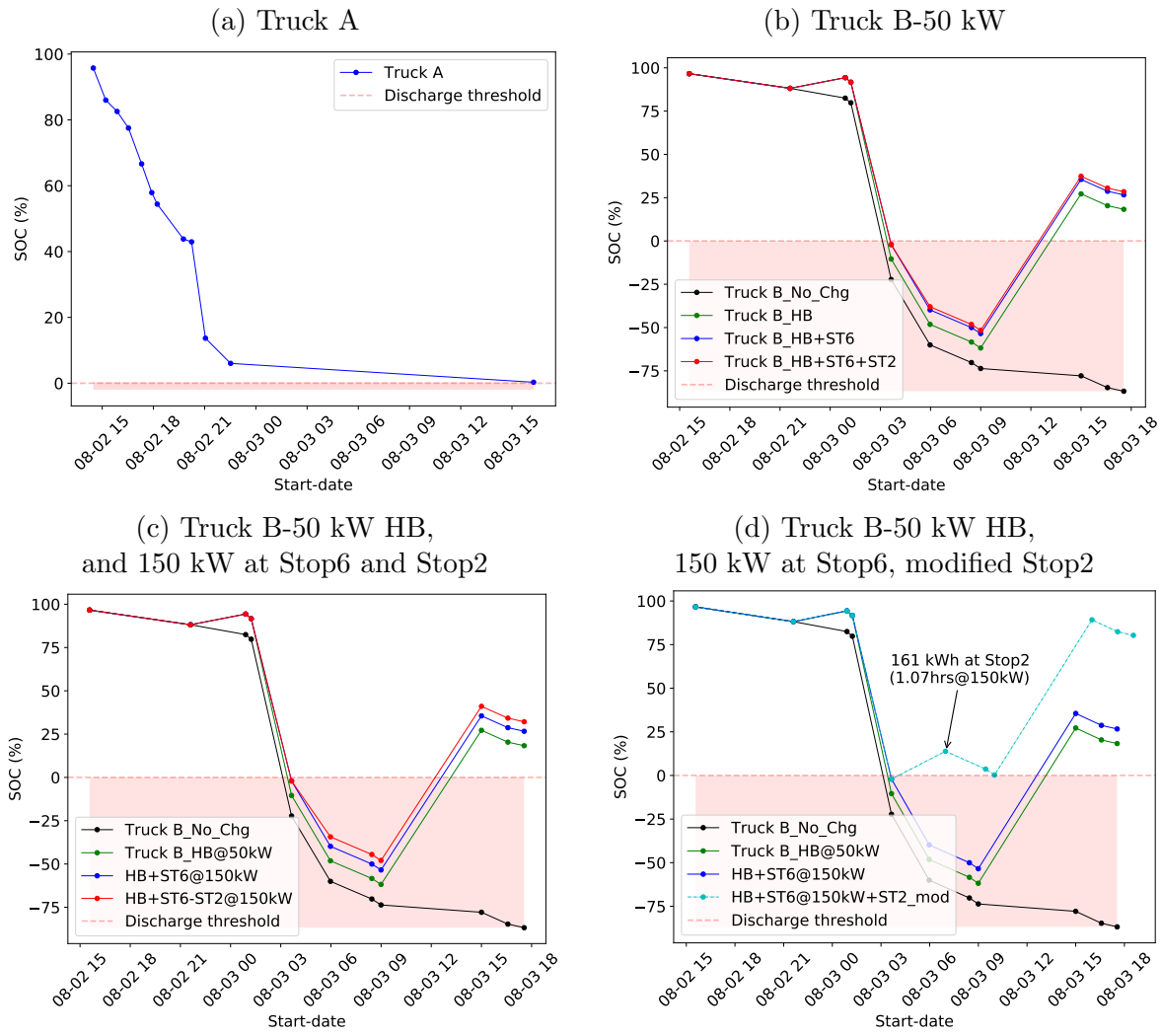

Figure 4.19: SOC scenario for Truck A from August 2-3 2021 (a). SOC scenarios for Truck B from August 2-3 2021 using a 50 kW charger (b). SOC scenarios for Truck B from August 2-3 2021 using a 50 kW charger at home-base and 150 kW charger at Stop6 and Stop2 (c). SOC scenarios for Truck B from August 2-3 2021 using a $50kW$ charger at home-base, 150 kW charger at Stop6, and 150 kW at Stop2 but extending its stay from 0.11 to 1.07 hours adding 161 kWh (d). Shaded red area represents the discharge threshold (HB=home-base, No_Chg=No Charging, ST6=Stop 6, ST2=Stop 2, ST2_mod= Stop 2 modified).

Chapter 5

Conclusions and Future Work

5.1 Conclusions

The main contribution of the dissertation lies in the development of innovative charging solutions for EVs, particularly addressing gaps in the literature related to EV charging pricing strategies and intelligent charging models for HD trucks. It proposes a data-driven, dynamic carbon-based pricing strategy to encourage EV charging during times of renewable energy surplus, thereby aligning EV charging with renewable energy production and local grid needs. Additionally, the dissertation investigates the impact of BET charging loads on the electric power grid, laying the groundwork for future research and the development of intelligent charging systems that could lead to a more sustainable and efficient use of energy resources in the transportation sector.

Specifically, this dissertation has presented the following achievements:

- Introduction of a real-time, data-driven carbon-based pricing model tailored for EV

charging. This model prioritizes periods of high renewable energy availability and integrates considerations of local solar PV variations, building power dynamics, and a TOU pricing framework. Furthermore, it leverages ML to achieve day-ahead and three-hour-ahead forecasts, identifying specific energy consumption patterns.

- Comprehensive analysis of trip-and-tour patterns shown by BETs in drayage operations at the San Pedro Bay ports. Through data-driven clustering techniques, energy efficiency—based on whether the vehicles are loaded or unloaded—has been adapted from current literature. This adaptation has been key in gaining valuable insights into the activity patterns of these trucks. Our simulations, which explored various charging scenarios, have provided a significant understanding of the SOC, particularly when considering potential en-route opportunity charging at designated power levels.

- Development of a cutting-edge, intelligently controlled charging model for BETs, made with the dual goals of maximizing tour completion while minimizing charging costs, all within the constraints of TOU energy rates. The efficacy of this model was underscored by a one year evaluation of real activity data from a fleet operating at the Ports of Los Angeles and Long Beach. To demonstrate its robustness, we conducted a sensitivity analysis comparing reserved SOC scenarios of 5%, 50%, and 80%.

5.2 Future Work

While this dissertation has produced many positive outcomes, there are still several unresolved problems that future work should address, especially in the area of intelligent charging and pricing strategies for electric vehicle fleets, particularly for MD and HD vehi-

cles.

First, data-driven carbon-based pricing could shift loads and incentivize smart charging behavior, supported further by policy, regulatory, and societal efforts. One potential future direction could involve introducing a grid resiliency fee to enhance the grid's robustness and security. Additionally, a net surplus rate might compensate for Net Energy Metering (NEM) tariffs when onsite-produced electricity exceeds the on-site load. Another avenue for exploration might be the integration of additional data sources into the ML model, such as battery storage rack data and EV charging statistics. A test bed could be established to incorporate the carbon-based pricing forecast into the level-2 EV chargers located at CE-CERT to evaluate this pricing strategy. The ultimate objective would be to assess changes in driver charging behavior by studying their willingness to pay.

Second, for a deeper understanding of electrification in MD and HD vehicles, it is crucial to identify trip-and-tour activity patterns and simulate en-route opportunity charging scenarios. One possible future direction is expanding the analysis to different fleets. Utilizing a global set of stops for the entire truck fleet can help in exploring alternative charging solutions and understanding queuing activity patterns, which are vital steps moving forward. Lastly, the strategic location of charging stations should be evaluated to determine which stops need conversion to electric vehicle charging stations, ensuring the optimal operation of battery electric drayage trucks and infrastructure planning.

Finally, it is clear that a substantial portion of drayage truck tours will require additional solutions for a successful electrified transition. Future modeling might contemplate BETs with extended ranges, introduce faster charging mechanisms, and re-route BETs to

account for their driving range as well as the necessary charging durations for subsequent tour completions. Moreover, addressing existing gaps and creating models for more precise estimates of trip-and-tour energy consumption are essential. The model proposed in this dissertation lays the groundwork for intelligent charging solutions tailored for BETs, aligning with California's vision for zero-emission drayage trucks. As this model continues to evolve, it should accommodate more fleet scenarios. The scope of analysis could also broaden to encompass factors such as temperature conditions, battery degradation, and battery cell imbalances, providing a more comprehensive perspective.

5.3 Selected Publications Resulting from this Research

[1] J. Garrido et al., "An Intelligently Controlled Charging Model for Battery Electric Trucks in Drayage Operations". *IEEE Transactions on Vehicular Technology (Under review).*

[2] J. Garrido, E. Hidalgo, M. Barth and K. Boriboonsomsin,"Home-Base Charging Load Profiles of Battery Electric Trucks Considering Tour Completion and Time-of-Use Rates," *2023 IEEE Transportation Electrification Conference & Expo (ITEC)*, Detroit, MI, USA, 2023, pp. 1-5, doi: 10.1109/ITEC55900.2023.10187064. [102]

[3] J. Garrido, E. Hidalgo, M. Barth and K. Boriboonsomsin, "En-Route Opportunity Charging for Heavy-Duty Battery Electric Trucks in Drayage Operations: Case Study at the Southern California Ports," *2022 IEEE Vehicle Power and Propulsion Conference (VPPC)*, Merced, CA, USA, 2022, pp. 1-6, doi: 10.1109/55846.2022.10003273.[95]

[4] J. Garrido et al., "Dynamic Data-Driven Carbon-Based Electric Vehicle Charging Pricing Strategy Using Machine Learning," *2021 IEEE International Intelligent Transportation Systems Conference (ITSC)*, Indianapolis, IN, USA, 2021, pp. 1670-1675, doi: 10.1109/ITSC48978.2021.9565130. [103]

Co-author:

[5] J. Yusuf, A. S. M. J. Hasan, J. Garrido, S. Ula, and M. J. Barth, "A comparative techno-economic assessment of bidirectional heavy duty and light duty plug-in electric vehicles operation: A case study," *Sustainable Cities and Society*, vol. 95, p. 104582, 2023.DOI:10.1016/j.scs.2023.10 [104]

[6] E. H. Gonzalez, J. Garrido, M. Barth and K. Boriboonsomsin, "Machine Learning-based Energy Consumption models for Battery Electric Trucks," *2023 IEEE Transportation Electrification Conference & Expo (ITEC)*, Detroit, MI, USA, 2023, pp. 1-6, doi: 10.1109/ITEC55900.2023.10187000. [105]

[7] Z. Bai, J. G. Escobar, G. Wu and M. J. Barth, "Object Perception Framework for Connected and Automated Vehicles: A Case Study," *2023 IEEE Transportation Electrification Conference & Expo (ITEC)*, Detroit, MI, USA, 2023, pp. 1-5, doi: 10.1109/ITEC55900.2023.10186931.[106]

[8] L. Fernando Enriquez-Contreras, A. S. M. Jahid Hasan, J. Yusuf, J. Garrido and S. Ula, "Microgrid Demand Response: A Comparison of Simulated and Real Results," *2022 North American Power Symposium (NAPS)*, Salt Lake City, UT, USA, 2022, pp. 1-6, doi: 10.1109/NAPS56150.2022.10012248.[107]

5.3.1 Invited Seminars

2023 MIT Energy Initiative, September 21, 2023, *"An Intelligently Controlled Charging Model for Battery Electric Trucks"*.

2023 Stanford University, Stanford Energy Control Lab , September 26, 2023, *"An Intelligently Controlled Charging Model for Battery Electric Trucks"*

2021 Climate Solutions Now Conference, October 2-3, 2021, Cal Poly San Luis Obispo, *"An Overview on Medium- and Heavy-Duty Vehicle Transportation Electrification Efforts and Renewable Energy Grid Integration"*.

Bibliography

[1] California air resources board (carb). 2022 inventory of greenhouse gas emissions. https://ww2.arb.ca.gov/ghg-inventory-data. Date accessed: October 2023.

[2] Weight classes categories from the united states department of energy. https://afdc.energy.gov/data/10380. Date accessed: October 2023.

[3] Types of vehicles by weight class from the united states department of energy. https://afdc.energy.gov/data/10381. Date accessed: October 2023.

[4] Carb-2020 mobile source strategy report. https://ww2.arb.ca.gov/sites/default/files/2021-04/Revised_Draft_2020_Mobile_Source_Strategy.pdf. Date accessed: October 2023.

[5] Shashank Arora, Alireza Tashakori Abkenar, Shantha Gamini Jayasinghe, and Kari Tammi. Chapter 6 - charging technologies and standards applicable to heavy-duty electric vehicles. In Shashank Arora, Alireza Tashakori Abkenar, Shantha Gamini Jayasinghe, and Kari Tammi, editors, *Heavy-Duty Electric Vehicles*, pages 135–155. Butterworth-Heinemann, 2021.

[6] Volvo electric truck. https://www.volvotrucks.us/trucks/vnr-electric/. Date accessed: October 2023.

[7] A review of wireless power transfer for electric vehicles: Prospects to enhance sustainable mobility. *Applied Energy*, 179:413–425, 2016.

[8] Southern california edison time-of-use (tou) rate periods. https://www.sce.com/business/rates/time-of-use. Date accessed: October 2023.

[9] Medium heavy duty electric transportation rate designs at sce. https://www.law.berkeley.edu/wp-content/uploads/2019/06/Session-3-Medium-Heavy-Duty-Transportation-Rate-Designs-at-SCE.pdf. Date accessed: October 2023.

[10] Inventory of u.s. greenhouse gas emissions and sinks. https://www.epa.gov/ghgemissions/inventory-us-greenhouse-gas-emissions-and-sinks. Date accessed: October 2023.

[11] O'dea, jimmy. 2019. ready for work: Now is the time for heavy-duty electric vehicles. cambridge, ma: Union of concerned scientists. https://www.ucsusa.org/resources/ready-work. Date accessed: October 2023.

[12] California air resources board. https://ww2.arb.ca.gov/resources/fact-sheets/governor-newsoms-zero-emission-2035-executive-order-n-79-20. Date accessed: October 2023.

[13] A.b. 1389, 2022 reyes, clean transportation program: project funding preferences, (ca. 2022).

[14] Federal highway administration. annual vehicle distance traveled in miles and related data - 2019 by highway category and vehicle type. https://www.fhwa.dot.gov/policyinformation/statistics/2021/vm1.cfm. Date accessed: October 2023.

[15] Aceee (american council for an energy-efficient economy): The state transportation electrification scorecard). https://www.aceee.org/research-report/t2301. Date accessed: October 2023.

[16] S.b. 32, 2006 pavley, california global warming solutions act of 2006: emissions limit.

[17] Executive order s-3-05. https://www.library.ca.gov/wp-content/uploads/GovernmentPublications/executive-order-proclamation/5129-5130.pdf. Date accessed: October 2023.

[18] Executive order b-16-2012. https://www.ca.gov/archive/gov39/2012/03/23/news17472/index.html. Date accessed: October 2023.

[19] Crisostomo Noel, Wendell Krell, Jeffrey Lu, , and Raja Ramesh. 2127 electric vehicle charging infrastructure assessment: Analyzing charging needs to support zero-emission vehicles in 2030. *California Energy Commission*, January 2021.

[20] Zero-emission drayage trucks challenges and opportunities for the san pedro bay ports. ucla luskin center for innovation. https://innovation.luskin.ucla.edu/wp-content/uploads/2019/10/Zero_Emission_Drayage_Trucks.pdf. Date accessed: October 2023.

[21] Chirag Panchal, Sascha Stegen, and Junwei Lu. Review of static and dynamic wireless electric vehicle charging system. *Engineering Science and Technology, an International Journal*, 21(5):922–937, 2018.

[22] Drive clean california. https://driveclean.ca.gov/electric-car-charging. Date accessed: October 2023.

[23] What is level 1, 2, 3 charging? https://www.cars.com/articles/what-is-level-1-2-3-charging-437766/. Date accessed: October 2023.

[24] Songyan Niu, Haiqi Xu, Zhirui Sun, Z.Y. Shao, and Linni Jian. The state-of-the-arts of wireless electric vehicle charging via magnetic resonance: principles, standards and core technologies. *Renewable and Sustainable Energy Reviews*, 114:109302, 2019.

[25] Ample. https://ample.com/. Date accessed: October 2023.

[26] Startup ample launches new battery swap for evs that could avoid the failures of previous ventures. https://www.forbes.com. Date accessed: October 2023.

[27] Veda Prakash Galigekere, Jason Pries, Omer C. Onar, Gui-Jia Su, Saeed Anwar, Randy Wiles, Larry Seiber, and Jonathan Wilkins. Design and implementation of an optimized 100 kw stationary wireless charging system for ev battery recharging. In *2018 IEEE Energy Conversion Congress and Exposition (ECCE)*, pages 3587–3592, 2018.

[28] Longzhao Sun, Dianguang Ma, and Houjun Tang. A review of recent trends in wireless power transfer technology and its applications in electric vehicle wireless charging. *Renewable and Sustainable Energy Reviews*, 91:490–503, 2018.

[29] James Druitt and Wolf-Gerrit Früh. Simulation of demand management and grid balancing with electric vehicles. *Journal of Power Sources*, 216:104 – 116, 2012.

[30] Thomas P. Lyon, Mark Michelin, Arie Jongejan, and Thomas Leahy. Is "smart charging" policy for electric vehicles worthwhile? *Energy Policy*, 41:259–268, 2012. Modeling Transport (Energy) Demand and Policies.

[31] P Florian Hacker, Ralph Harthan, Felix Matthes, and Wiebke Zimmer. Environmental impacts and impact on the electricity market of a large scale introduction of electric cars in europe. 2009.

[32] Joyce McLaren, John Miller, Eric O'Shaughnessy, Eric Wood, and Evan Shapiro. Co2 emissions associated with electric vehicle charging: The impact of electricity generation mix, charging infrastructure availability and vehicle type. *The Electricity Journal*, 29(5):72 – 88, 2016.

[33] K. Parks, P. Denholm, and T. Markel. Costs and emissions associated with plug-in hybrid electric vehicle charging in the xcel energy colorado service territory. *National Renewable Energy Laboratory*, 2007.

[34] Bogdan Ovidiu Varga. Electric vehicles, primary energy sources and co2 emissions: Romanian case study. *Energy*, 49:61–70, 2013.

[35] Federico Millo, Luciano Rolando, Rocco Fuso, and Fabio Mallamo. Real co2 emissions benefits and end user's operating costs of a plug-in hybrid electric vehicle. *Applied Energy*, 114:563 – 571, 2014.

[36] Patrick Jochem, Sonja Babrowski, and Wolf Fichtner. Assessing co2 emissions of electric vehicles in germany in 2030. *Transportation Research Part A: Policy and Practice*, 78:68 – 83, 2015.

[37] T. Donateo, F. Licci, A. D'Elia, G. Colangelo, D. Laforgia, and F. Ciancarelli. Evaluation of emissions of co2 and air pollutants from electric vehicles in italian cities. *Applied Energy*, 157:675 – 687, 2015.

[38] Reed T. Doucette and Malcolm D. McCulloch. Modeling the co2 emissions from battery electric vehicles given the power generation mixes of different countries. *Energy Policy*, 39(2):803–811, 2011. Special Section on Offshore wind power planning, economics and environment.

[39] Lluc Canals Casals, Egoitz Martinez-Laserna, Beatriz Amante García, and Nerea Nieto. Sustainability analysis of the electric vehicle use in europe for co2 emissions reduction. *Journal of Cleaner Production*, 127:425–437, 2016.

[40] Nicolò Daina, Aruna Sivakumar, and John W. Polak. Electric vehicle charging choices: Modelling and implications for smart charging services. *Transportation Research Part C: Emerging Technologies*, 81:36 – 56, 2017.

[41] M. Wolinetz, J. Axsen, J. Peters, and C. Crawford. Simulating the value of electric-vehicle–grid integration using a behaviourally realistic model. *Nature Energy*, 3:132–139, 02 2018.

[42] HyungBin Moon, Stephen Youngjun Park, Changhyun Jeong, and Jongsu Lee. Forecasting electricity demand of electric vehicles by analyzing consumers' charging patterns. *Transportation Research Part D: Transport and Environment*, 62:64 – 79, 2018.

[43] Sulabh Sachan and Nadia Adnan. Stochastic charging of electric vehicles in smart power distribution grids. *Sustainable Cities and Society*, 40:91 – 100, 2018.

[44] George Hilton, Thomas Bryden, Carlos Ponce de Leon, and Andrew Cruden. Dynamic charging algorithm for energy storage devices at high rate ev chargers for integration of solar energy. *Energy Procedia*, 151:2 – 6, 2018. 3rd Annual Conference in Energy Storage and Its Applications, 3rd CDT-ESA-AC, 11–12 September 2018, The University of Sheffield, UK.

[45] G. Wang, V. Disfani, and J. Kleissl. Scenario based stochastic optimization of probabilistic ev charging scheduling. In *2018 IEEE Innovative Smart Grid Technologies - Asia (ISGT Asia)*, pages 552–557, 2018.

[46] Guang Chao Wang, Elizabeth Ratnam, Hamed Valizadeh Haghi, and Jan Kleissl. Corrective receding horizon ev charge scheduling using short-term solar forecasting. *Renewable Energy*, 130:1146 – 1158, 2019.

[47] Colin J. R. Sheppard, Alan T. Jenn, Jeffery B. Greenblatt, Gordon S. Bauer, and Brian F. Gerke. Private versus shared, automated electric vehicles for u.s. personal mobility: Energy use, greenhouse gas emissions, grid integration, and cost impacts. *Environmental Science & Technology*, 0(0):null, 0. PMID: 33566604.

[48] Md Shariful Islam and N. Mithulananthan. Pv based ev charging at universities using supplied historical pv output ramp. *Renewable Energy*, 118:306 – 327, 2018.

[49] Md Shariful Islam, Nadarajah Mithulananthan, and Duong Quoc Hung. Coordinated ev charging for correlated ev and grid loads and pv output using a novel, correlated,

probabilistic model. *International Journal of Electrical Power & Energy Systems*, 104:335 – 348, 2019.

[50] James Dixon, Waqquas Bukhsh, Calum Edmunds, and Keith Bell. Scheduling electric vehicle charging to minimise carbon emissions and wind curtailment. *Renewable Energy*, 161:1072–1091, 2020.

[51] Chargepoint station owner support. `https://www.chargepoint.com/products/support-faq/`. Date accessed: October 2023.

[52] Chargepoint find a station. `https://na.chargepoint.com/charge_point`. Date accessed: October 2023.

[53] Electrify america. `https://www.electrifyamerica.com/pricing/`. Date accessed: October 2023.

[54] California department of food and agriculture division of measurement standards electric vehicle supply equipment (evse). `https://www.cdfa.ca.gov/dms/programs/zevfuels/`. Date accessed: October 2023.

[55] Kai Yuan, Yi Song, Yinchi Shao, Chongbo Sun, and Zhili Wu. A charging strategy with the price stimulus considering the queue of charging station and ev fast charging demand. *Energy Procedia*, 145:400 – 405, 2018. Renewable Energy Integration with Mini/Microgrid.

[56] Zachary J. Lee, John Z.F. Pang, and Steven H. Low. Pricing ev charging service with demand charge. *Electric Power Systems Research*, 189:106694, 2020.

[57] W. Ji, K. Yu, X. Chen, and L. Gan. Research on pricing strategy of ev charging load agent in residential areas considering peak-shifting and valley-filling. In *2019 IEEE 3rd Conference on Energy Internet and Energy System Integration (EI2)*, pages 677–682, 2019.

[58] C. Latinopoulos, A. Sivakumar, and J.W. Polak. Response of electric vehicle drivers to dynamic pricing of parking and charging services: Risky choice in early reservations. *Transportation Research Part C: Emerging Technologies*, 80:175 – 189, 2017.

[59] X. Chen, C. Tan, S. Kiliccote, and R. Rajagopal. Electric vehicle charging during the day or at night? a perspective on carbon emissions. In *2019 IEEE Power Energy Society General Meeting (PESGM)*, pages 1–5, 2019.

[60] Xiaohong Dong, Yunfei Mu, Xiandong Xu, Hongjie Jia, Jianzhong Wu, Xiaodan Yu, and Yan Qi. A charging pricing strategy of electric vehicle fast charging stations for the voltage control of electricity distribution networks. *Applied Energy*, 225:857–868, 2018.

[61] Chao Wang, Peng Hao, Kanok Boriboonsomsin, and Matthew Barth. Developing a mesoscopic energy consumption model for battery electric trucks using real-world diesel truck driving data. In *2022 IEEE Vehicle Power and Propulsion Conference (VPPC)*, pages 1–6, 2022.

[62] Lalit Patnaik, Phuoc Sang Huynh, Deepa Vincent, and Sheldon S. Williamson. Wireless opportunity charging as an enabling technology for ev battery size reduction and range extension: Analysis of an urban drive cycle scenario. In *2018 IEEE PELS Workshop on Emerging Technologies: Wireless Power Transfer (Wow)*, pages 1–5, 2018.

[63] Zero-emission catenary hybrid truck market study. `https://www.gladstein.org/gna_whitepapers/zero-emission-catenary-hybrid-truck-market-study/`. Date accessed: October 2023.

[64] One way to curb freight emissions: Put trucks on an electric catenary system. `https://arstechnica.com`. Date accessed: October 2023.

[65] Key performance parameters for drayage trucks operating at the ports of los angeles and long beach. calstart. `https://calstart.org/wp-content/uploads/2018/10/I-710-Project_Key-Performance-Parameters-for-Drayage-Trucks.pdf`. Date accessed: October 2023.

[66] Hanjiro Ambrose. Electrification of drayage trucks: On track for a sustainable freight path. 01 2016.

[67] Shams Tanvir, Fuad Un-Noor, Kanok Boriboonsomsin, and Zhiming Gao. Feasibility of operating a heavy-duty battery electric truck fleet for drayage applications. *Transportation Research Record Journal of the Transportation Research Board*, 2675, 11 2020.

[68] Rajeev Namboothiri and Alan L. Erera. Planning local container drayage operations given a port access appointment system. *Transportation Research Part E: Logistics and Transportation Review*, 44(2):185–202, 2008. Selected Papers from the National Urban Freight Conference.

[69] Frederik Schulte, Rosa Gonzalez Ramirez, and Stefan Voss. Reducing port-related truck emissions: Coordinated truck appointments to reduce empty truck trips. volume 9335, pages 495–509, 09 2015.

[70] Edward McCormack and Mark E. Hallenbeck. Its devices used to collect truck data for performance benchmarks. *Transportation Research Record*, 1957(1):43–50, 2006.

[71] Xiaolei Ma, Edward D. McCormack, and Yinhai Wang. Processing commercial global positioning system data to develop a web-based truck performance measures program. *Transportation Research Record*, 2246(1):92–100, 2011.

[72] Soyoung Iris You and Stephen G. Ritchie. Gps data processing framework for analysis of drayage truck tours. *KSCE Journal of Civil Engineering*, 22, 2018.

[73] Maleki Mina Kargar Mehdi Chen Jessica Maoh Hanna Patel, Vidhi. A cluster-driven classification approach to truck stop location identification using passive gps data. *Journal of Geographical Systems*, 24, 2022.

[74] Xiangqi Zhu, Barry Mather, and Partha Mishra. Grid impact analysis of heavy-duty electric vehicle charging stations. In *2020 IEEE Power Energy Society Innovative Smart Grid Technologies Conference (ISGT)*, pages 1–5, 2020.

[75] Kyrre Kirkbakk Fjær, Venkatachalam Lakshmanan, Bendik Nybakk Torsæter, and Magnus Korpås. Heavy-duty electric vehicle charging profile generation method for grid impact analysis. In *2021 International Conference on Smart Energy Systems and Technologies (SEST)*, pages 1–6, 2021.

[76] Brennan Borlaug, Matteo Muratori, Madeline Gilleran, David Woody, William Muston, Thomas Canada, Andrew Ingram, Hal Gresham, and Charlie McQueen. Heavy-duty truck electrification and the impacts of depot charging on electricity distribution systems. *Nature Energy*, 6(6):673–682, Jun 2021.

[77] Rayan El Helou, S. Sivaranjani, Dileep Kalathil, Andrew Schaper, and Le Xie. The impact of heavy-duty vehicle electrification on large power grids: A synthetic texas case study. *Advances in Applied Energy*, 6:100093, 2022.

[78] Fan Tong et al. Energy consumption and charging load profiles from long-haul truck electrification in the united states. *Environmental Research: Infrastructure and Sustainability*, 1:025007, 2021.

[79] Bassam Al-Hanahi, Iftekhar Ahmad, Daryoush Habibi, and Mohammad A.S. Masoum. Smart charging strategies for heavy electric vehicles. *eTransportation*, 13:100182, 2022.

[80] Yanbiao Feng and Zuomin Dong. Optimal energy management with balanced fuel economy and battery life for large hybrid electric mining truck. *Journal of Power Sources*, 454:227948, 2020.

[81] Mohammed Al-Saadi, Josu Olmos, Andoni Saez-de Ibarra, Joeri Van Mierlo, and Maitane Berecibar. Fast charging impact on the lithium-ion batteries' lifetime and cost-effective battery sizing in heavy-duty electric vehicles applications. *Energies*, 15(4):1278, Feb 2022.

[82] Björn Nykvist and Olle Olsson. The feasibility of heavy battery electric trucks. *Joule*, 5(4):901–913, 2021.

[83] California air resources board, carbon allowance prices auction dates. `https://ww2.arb.ca.gov/our-work/programs/cap-and-trade-program/auction-information/auction-notices-and-reports`. Date accessed: October 2023.

[84] California air resources board, carbon allowance prices. `https://ww2.arb.ca.gov/sites/default/files/2020-09/carbonallowanceprices_0.pdf`. Date accessed: October 2023.

[85] Riverside public utilities, electricity rates. `https://riversideca.gov/utilities/residents/rates/electric-rules-rates`. Date accessed: October 2023.

[86] Riverside public utilities, electricity rates large general and industrial service. https://riversideca.gov/utilities/sites/riversideca.gov.utilities/files/pdf/rates-electric/Electric%20Schedule%20TOU%20-%20Effective%2001-1-19.pdf. Date accessed: October 2023.

[87] Greenhouse gas emission tracking methodology. https://www.caiso.com/Documents/GreenhouseGasEmissionsTracking-Methodology.pdf. Date accessed: October 2023.

[88] Random forest regression. https://levelup.gitconnected.com/random-forest-regression-209c0f354c84. Date accessed: October 2023.

[89] D. Su, E. Batzelis, and B. Pal. Machine learning algorithms in forecasting of photovoltaic power generation. In *2019 International Conference on Smart Energy Systems and Technologies (SEST)*, pages 1–6, 2019.

[90] Scikit learn. https://scikit-learn.org/stable/modules/generated/sklearn.ensemble.RandomForestRegressor.html. Date accessed: October 2023.

[91] U.s department of energy. https://afdc.energy.gov/fuels/electricity_charging_home.html. Date accessed: October 2023.

[92] Bryce W. Sharman and Matthew J. Roorda. Analysis of freight global positioning system data: Clustering approach for identifying trip destinations. *Transportation Research Record*, 2246(1):83–91, 2011.

[93] The elbow method. https://www.oreilly.com/library/view/statistics-for-machine/9781788295758/c71ea970-0f3c-4973-8d3a-b09a7a6553c1.xhtml. Date accessed: October 2023.

[94] Clustering: K-means. https://www.codecademy.com/learn/machine-learning/modules/dspath-clustering/cheatsheet. Date accessed: October 2023.

[95] Jacqueline Garrido, Emmanuel Hidalgo, Matthew Barth, and Kanok Boriboonsomsin. En-route opportunity charging for heavy-duty battery electric trucks in drayage operations: Case study at the southern california ports. In *2022 IEEE Vehicle Power and Propulsion Conference (VPPC)*, pages 1–6, 2022.

[96] Matt Miyasato and Phil Barroca. Zero emission drayage trucks demonstration (zect 1) (final report). 3 2020.

[97] Fuad Un-Noor, Alexander Vu, Shams Tanvir, Zhiming Gao, Matt Barth, and Kanok Boriboonsomsin. Range extension of battery electric trucks in drayage operations with wireless opportunity charging at port terminals. In *2022 IEEE Vehicle Power and Propulsion Conference (VPPC)*, pages 1–6, 2022.

[98] Pulp 2.7.0. https://pypi.org/project/PuLP/. Date accessed: September 2023.

[99] Scipy.optimize. https://docs.scipy.org/doc/scipy/reference/optimize.html. Date accessed: September 2023.

[100] The economic costs of freight transportation. `https://ops.fhwa.dot.gov/freight/freight_analysis/freight_story/costs.htm`. Date accessed: October 2023.

[101] Take charge: A guidebook to fleet electrification and infrastructure. `https://www.sce.com/sites/default/files/2020-07/Electrification%20%26%20Infrastructure%20Guidebook-Final_06.29.20.pdf`. Date accessed: October 2023.

[102] Jacqueline Garrido, Emmanuel Hidalgo, Matthew Barth, and Kanok Boriboonsomsin. Home-base charging load profiles of battery electric trucks considering tour completion and time-of-use rates. In *2023 IEEE Transportation Electrification Conference Expo (ITEC)*, pages 1–5, 2023.

[103] Jacqueline Garrido, Matthew J. Barth, Luis Enriquez-Contreras, ASM Jahid Hasan, Michael Todd, Sadrul Ula, and Jubair Yusuf. Dynamic data-driven carbon-based electric vehicle charging pricing strategy using machine learning. In *2021 IEEE International Intelligent Transportation Systems Conference (ITSC)*, pages 1670–1675, 2021.

[104] Jubair Yusuf, A S M Jahid Hasan, Jacqueline Garrido, Sadrul Ula, and Matthew J. Barth. A comparative techno-economic assessment of bidirectional heavy duty and light duty plug-in electric vehicles operation: A case study. *Sustainable Cities and Society*, 95:104582, 2023.

[105] Emmanuel Hidalgo Gonzalez, Jacqueline Garrido, Matthew Barth, and Kanok Boriboonsomsin. Machine learning-based energy consumption models for battery electric trucks. In *2023 IEEE Transportation Electrification Conference Expo (ITEC)*, pages 1–6, 2023.

[106] Zhengwei Bai, Jacqueline Garrido Escobar, Guoyuan Wu, and Matthew J. Barth. Object perception framework for connected and automated vehicles: A case study. In *2023 IEEE Transportation Electrification Conference Expo (ITEC)*, pages 1–5, 2023.

[107] Luis Fernando Enriquez-Contreras, A S M Jahid Hasan, Jubair Yusuf, Jacqueline Garrido, and Sadrul Ula. Microgrid demand response: A comparison of simulated and real results. In *2022 North American Power Symposium (NAPS)*, pages 1–6, 2022.